Int. J. Heat Mass Transfer. Vol. 2, pp. 283–313. Pergamon Press 1961. Printed in Great Britain.

THE PREDICTION OF MASS TRANSFER RATES WHEN EQUILIBRIUM DOES NOT PREVAIL AT THE PHASE INTERFACE*

D. B. SPALDING
Imperial College, London, S.W.7

(*Received August*, 1960)

Abstract—It is shown that departures from thermodynamic equilibrium at the interface call for only small modifications in standard procedures for calculating mass transfer rates. If enthalpy–composition diagrams are used for representing thermodynamic properties and evaluating mass transfer driving forces, the modifications comprise the replacement of the single curve, valid for equilibrium mixtures in contact with the neighbouring phase, by a family of curves; the parameter of this family is the ratio of the mass transfer conductance to a molecular flux.

These and other aspects of mass transfer theory are illustrated by reference to: the vaporization of water into air; the combustion of carbon in air; the pyrolysis of a solid or liquid without chemical reaction; and the combustion of a pellet of ammonium perchlorate in a stream of fuel gas. The examples discussed numerically relate to axi-symmetrical stagnation point flows with laminar boundary layers.

Résumé—Quand on s'éloigne de l'équilibre thermodynamique qui règne dans la zone de séparation de deux phases les modifications à apporter au calcul classique du transport de matière sont peu importantes. Si les diagrammes enthalpiques sont utilisés pour la représentation des propriétés thermodynamiques et l'évaluation des forces provoquant le transport de masse, les corrections consistent à remplacer la courbe unique valable pour les mélanges en équilibre au voisinage de la phase, par une famille de courbes; le paramètre de cette famille est la rapport du transport de masse au flux moléculaire.

Ces aspects de la théorie du transport de masse sont illustrés par: la vaporisation de l'eau dans l'air, la combustion du carbone dans l'air, la pyrolyse d'un solide ou d'un liquide sans réaction chimique et la combustion d'un grain de perchlorate d'ammonium dans un courant de gaz combustible.

Les exemples numériques étudiés sont relatifs à des écoulements de révolution avec couches limites laminaires.

Zusammenfassung—Es wird gezeigt, dass Abweichungen vom thermodynamischen Gleichgewicht an der Zwischenfläche nur geringe Änderungen der üblichen Berechnungsmethoden der Stoffübertragung verlangen. Soweit die thermodynamischen Eigenschaften in Enthalpie-Diagrammen dargestellt sind und danach die treibenden Kräfte des Stoffaustausches beurteilt werden, genügt es, die für Gleichgewichtsmischungen in Berührung mit der benachbarten Phase gültige Einzelkurve durch eine Kurvenschar zu ersetzen. Der Parameter dieser Schar ist das Verhältnis von Mengenstromdichte zu einem Molekularfluss.

Diese und andere Gesichtspunkte der Theorie der Stoffübertragung werden an folgenden Beispielen erläutert: der Verdampfung von Wasser in Luft; der Verbrennung von Kohlenstoff in Luft; der thermischen Zersetzung eines Festkörpers oder einer Flüssigkeit ohne chemische Reaktion und der Verbrennung eines Kügelchens aus Ammoniumperchlorat in einem Brenngasstrom. Die numerisch ausgewerteten Beispiele beziehen sich auf achs-symmetrische Staupunktsströmungen mit laminarer Grenzschicht.

Аннотация—Если имеет место нарушение термодинамического равновесия на поверхности раздела фаз, то для расчёта потоков массы можно модифицировать обычные методы расчёта. Диаграммы энтальпии используются для изображения термодинамических характеристик и для численного выражения движущих сил массообмена, при этом единичная кривая, характерная для равновесных смесей, которые находятся в контакте с соседней фазой, заменяется на семейство кривых; параметром этого семейства является отношение коэффициента массообмена к молекулярному потоку.

* This work was performed in the author's capacity as consultant to the Lockheed Missiles and Space Division, Palo Alto, California. The work was financed by AFOSR Contract.

Высказанные положения теории массообмена иллюстрируются результатами исследования процессов: испарения воды в воздух, сгорания углерода в воздухе, пиролиза твёрдого или жидкого тела без химической реакции и горения частицы аммония перхлората в потоке топочного газа. Обсуждаемые примеры численно относятся к критической точке осесимметричных потоков с ламинарными пограничными слоями.

NOTATION

a_j = Velocity of sound in gas j (ft/h), (equation 23);

b = Dimensionless conserved property (—), (equation 5);

B = Driving force for mass transfer (—), (equation 13);

D = Diameter of nozzle (ft), (equation 1a);

E = Activation energy (Btu/lb mole), (equation 31);

f = Mass fraction of one of two parent substances in a mixture (lb_m/lb_m), (equation 2a);

g = Mass-transfer conductance (lb_m/ft^2h), (equation 9);

G = Reference "mass velocity" (lb_m/ft^2h), (equation 10);

$\mathbf{G}$ = Mass-flux vector (lb_m/ft^2h), (equation 2);

h = Specific enthalpy of mixture (Btu/lb_m), (equation 2);

k_j = Specific heat ratio of gas j (—), (equation 23);

K_{ox} = Parameter measuring relative magnitude of mass-transfer conductance and oxygen collision rate (—), (equation 33);

K_{pyr} = Parameter measuring relative magnitude of mass-transfer conductance and surface-pyrolysis rate (—), (equation 37);

K_{vap} = Parameter measuring relative magnitude of mass-transfer conductance and vacuum vaporization rate (—), (equation 26).

m_j = Mass fraction of component j in mixture (lb_m/lb_m), (equation 24);

$\dot{m}''$ = Mass flux across phase interface into fluid under consideration (lb_m/ft^2h), (equation 3);

$\overleftarrow{\dot{m}_j''}$ = Mass rate of impingement of molecules of j from gas phase on condensed phase (lb_m/ft^2h), (equation 23);

$\overrightarrow{\dot{m}_j''}$ = Mass rate of flow of molecules from condensed phase into gas phase (lb_m/ft^2h), (equation 24);

Pr = Prandtl number (—), (equation 10);

$\dot{q}''$ = Heat flux (Btu/ft^2h), (equation 17);

r = Stoichiometric ratio (—), (equation 31);

$\mathscr{R}$ = Universal gas constant, = 1·98 (Btu/lb mole), (equation 31);

R_n = Radius of nose-cone (ft), (equation 1);

t = Temperature (°F);

T = Absolute temperature (°F abs.), (equation 31);

u = Gas velocity (ft/h), (equation 1);

x = Distance along surface in direction of main stream flow (ft), (equation 1);

y = Distance from interface towards fluid under consideration (ft), (equation 3);

Z_{pyr} = A constant in the pyrolysis (lb_m/ft^2h), (equation 35).

Greek symbols

α = Fraction of "sticky" collisions on a surface (—), (equation 24);

Γ = Exchange coefficient (thermal conductivity divided by specific heat or diffusion coefficient multiplied by density (lb_m/ft h), (equation 2);

η = Dimensionless enthalpy gradient (—), (equation 39);

μ = Absolute viscosity of fluid (lb_m/ft h), (equation 28);

ρ = Density of fluid (lb_m/ft^3), (equation 1);

σ = Stefan's Constant, = $0{\cdot}1713 \times 10^{-8}$ (Btu/ft^2h (°F abs.)^4), (equation 42).

Subscripts

G = Main stream state;

L = Fluid state in neighbouring phase adjacent interface;

O = Supply state;

S = Fluid state in considered phase adjacent interface;
T = Transferred-substance state;
G_L, G_S, T_L, T_S = See text, Section 2.2;
∞ = Far upstream;
rad = Radiation;
eq = Equilibrium;
ox = Oxidant;
ad = Adiabatic.

1. INTRODUCTION

1.1. *Problem considered*

THERE are many important practical processes in which mass transfer between two phases is accompanied by a chemical reaction between the transferred substance and the fluid stream into which it passes. Of these, several have been subjected to fairly complete study, for example—the combusion of liquid fuels [1]; the combustion of solid fuels [2]; burning of a transpiration-coolant [3].

The processes which have been most thoroughly studied heretofore are those in which the fluid adjacent to the phase interface can be assumed to be in a state of thermodynamic equilibrium: this assumption provides one boundary condition for the mathematical problem. In the present paper, therefore, attention is concentrated on those processes for which equilibrium does *not* prevail at the interface.

Examples of the latter type include—vaporization at very high rates but at low pressures; burning of a solid fuel (e.g. carbon) under conditions such that the chemical reaction rate is not "very fast"; the pyrolysis of the material of the "heat-shield" of a missile re-entering the earth's atmosphere; and the burning of an oxidant (e.g. ammonium perchlorate) pellet exposed to a stream of hydrocarbon gas.

All these examples will be discussed in the present paper.

1.2. *Purpose of the paper*

Problems of the present type have been discussed on many earlier occasions. To choose but one example, Tu *et al.* [4] made an experimental and theoretical study of the burning of a carbon surface in an air stream; this study spanned the whole range of conditions from those in which the diffusion boundary layer controlled the rate of burning (hot carbon surface) to those in which the chemical reaction-rate constants exerted a decisive control (colder carbon surface). Reviews of the relevant literature have been made by Spalding [5], Wicke [6], Khitrin [7] and others.

The purpose of the present work is not therefore to break fundamentally new ground, although perhaps it does so in the case of the ammonium perchlorate problem discussed below. Rather the purpose is to aid understanding of the processes in question, and simplify the theoretical prediction of the mass transfer rate in any particular case. This purpose is achieved by discussing the processes in question within the framework of a standard formulation of mass transfer processes in general [8]. In particular, it is desired to make clear that enthalpy–composition charts are as useful for the present class of processes as they have proved to be for processes in which thermodynamic equilibrium prevails at the interface, [2, 9, 10, 11, 12, 13, 14, 15].

An additional purpose of the paper is to apply the methods in question to laminar axi-symmetrical stagnation-point flows. There are two reasons: the first is that these flows are of great practical importance (for example at the nose of a missile); the second is that such flows are easily contrived in the laboratory, where they may provide the means by which reaction–kinetic constants can be deduced from measurements of mass transfer rates.

1.3. *The stagnation-point flow*

A description of two particular axi-symmetrical stagnation-point flows now follows, in order that a concrete physical situation and a definite theoretical question may be held in mind during the subsequent analysis. The majority of the analysis however (specifically, the calculation of the mass transfer *driving force*), is valid for *any* flow pattern adjacent the surface.

(i) *The nose-cone problem.* Fig. 1 illustrates the flow adjacent the nose-cone of a high-speed missile flying at supersonic speed. A shock wave is formed a short distance ahead of the solid surface; upstream of this wave the reactive gas velocity is axial, with value u_∞; downstream of the wave, the velocity has a predominantly

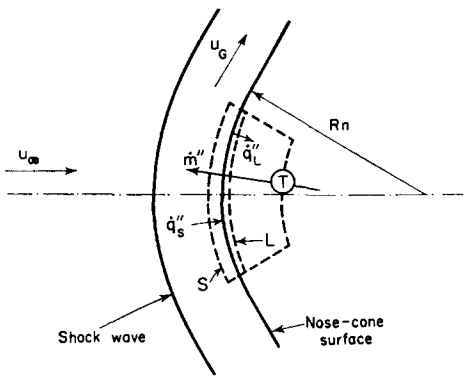

FIG. 1. Illustrating the laminar axi-symmetrical stagnation-point flow at the nose of a missile in high-speed flight.

radial direction and a magnitude (except within the boundary layer) of u_G. The latter quantity increases with distance x from the axis of symmetry in obedience (according to Li and Geiger [16]) to the relation:

$$\frac{u_G}{x} = \frac{du_G}{dx} = \frac{u_\infty}{R_n}\sqrt{\left(\frac{\rho_\infty}{\rho_G}\left\{2 - \frac{\rho_\infty}{\rho_G}\right\}\right)} \qquad (1)$$

where: R_n = radius of nose cone
ρ = gas density,
subscripts ∞ and G refer to conditions respectively upstream and downstream of the shock.

The central question to be considered is: What is the rate at which material is transferred into the gas phase by mass transfer? The symbol for the mass transfer rate is $\dot{m}''$; this quantity is also known as the "ablation rate" in missile engineering. The question will be seen to have three parts, namely: What are the influences on $\dot{m}''$ of the aerodynamic variables, i.e. u_∞, R_n, viscosity, density, etc.? What are the influences of the thermodynamic properties of the fluid stream and of the transferred material? And what are the influences of the reaction-kinetic constants of the chemical transformations which occur?

(ii) *The perpendicular-jet problem.* Fig. 2 illustrates a flow which may be used for the laboratory testing of materials. A jet of fluid, for example, oxygen at velocity u_∞, flows towards a perpendicular surface, which deflects the stream radially outward. The velocity field is somewhat more complex than that of Fig. 1;

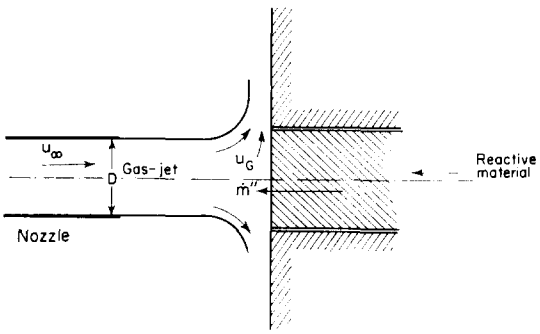

FIG. 2. Illustrating the axi-symmetrical stagnation-point flow resulting from the impingement of a jet on a perpendicular surface.

however, if u_G is again defined as the radial component of the velocity just outside the boundary layer which forms on the surface, we may write, [17],

$$\frac{u_G}{x} = \frac{du_G}{dx} \approx \frac{u_\infty}{D}. \qquad (1a)$$

Here x = distance from symmetry axis as before, and
D = jet diameter.

In some of the situations to which the present paper is relevant, at least the central portion of the solid surface will be composed of a material which reacts chemically, partially as a result of contact with the fluid stream. If steady conditions prevail, the reactive material must be supplied steadily so as to maintain its reacting surface at a fixed position. The question to which we address ourselves is this; at what rate must the material be supplied in order to maintain the steady state in given conditions, i.e. with fixed u_∞, D, materials, temperature and pressure?

1.4. *Outline of the present paper*

Section 2 describes the standard framework of convective mass transfer theory into which

it is desired to fit the processes under discussion. It is shown that, with certain restrictions, all mass transfer problems can be resolved into the determination of a conductance and the determination of a driving force.

Section 3 contains the description of methods for determining the values of the driving force, both in general and with particular examples. It is shown that problems of the present kind differ from those in which equilibrium prevails at the surface primarily in the location of a curve (the S-curve) on the relevant enthalpy–composition diagram. It is hoped that, although the substances mentioned by name are necessarily few in number, examination of the examples will make clear how other substances are to be handled theoretically.

Section 4 contains a résumé of methods for the calculation of the conductance for axi-symmetrical stagnation point flows. Together with the material of Section 3, this permits the discussion of particular processes in Section 5.

2. THE STANDARD FORMULATION

2.1. *Mathematics*

Equations. It has been shown by the present author* [8], that, provided that all "exchange coefficients" (thermal conductivity of the mixture divided by specific heat of the mixture at constant pressure; diffusion coefficient of each mixture component multiplied by mixture density) are numerically equal at each point in the mixing field, the enthalpy h and mass fraction f obey respectively the differential equations:

$$\boldsymbol{G}.(\nabla h) - \nabla\{(\Gamma(\nabla h)\} = 0 \qquad (2)$$

$$\boldsymbol{G}.(\nabla f) - \nabla\{(\Gamma(\nabla f)\} = 0 \qquad (2a)$$

where: $\boldsymbol{G}$ = mass flux vector (lb_m/ft^2h);
h = specific enthalpy of mixture (Btu/lb_m);
f = mass of material in unit mass of mixture which derives from one ("father") of the two ("parent") streams of fluid entering the mixing field, regardless of whether chemical transformations have occurred (lb_m/lb_m).
Γ = exchange coefficient† as defined above (lb_m/ft h).

Equations (2) and (2a) hold for steady flow at low Mach number.

Boundary conditions. The same reference shows that important boundary conditions for equations (2) and (2a) are as follows:

At a control surface S (Fig. 3), within the fluid under consideration and immediately

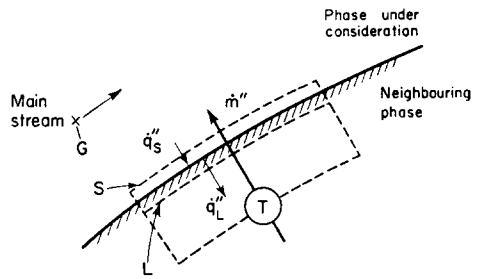

FIG. 3 Illustrating notation used in describing heat and mass transfer through a phase interface.

adjacent the interface across which mass transfer occurs:

$$\dot{m}'' = \frac{[\Gamma(\partial h/\partial y)]_S}{h_S - h_T} \qquad (3)$$

$$\dot{m}'' = \frac{[\Gamma(\partial f/\partial y)]_S}{f_S - f_T} \qquad (4)$$

where: $\dot{m}''$ = net mass flux through the surface towards the fluid under consideration (lb_m/ft^2h);
y = distance normal to the interface (ft);
Suffix S indicates evaluation at the S control surface;
Suffix T indicates evaluation for the "transferred substance state", so defined that:

$$h_T = h_{T_S} - \dot{q}''_S/\dot{m}''$$
$$= h_{T_L} - \dot{q}''_L/\dot{m}''$$

* The paper referred to gives a literature survey, indicating the contributions of other authors, as well as giving the derivation of the equations and their limits of validity.

† Γ can be regarded as dynamic viscosity μ divided by Prandtl or Schmidt number. It may vary with position.

h_{T_S} = enthalpy of transferred material as it crosses the S control surface (Btu/lb_m);

h_{T_L} = enthalpy of transferred material as it crosses the L control surface (Fig. 3) (Btu/lb_m);

$\dot{q}''_S$ = heat flux across S control surface (sign convention as indicated in Fig. 3) (Btu/ft^2h);

$\dot{q}''_L$ = heat flux across L control surface (sign convention as indicated in Fig. 3) (Btu/ft^2h);

$f_T \equiv \dot{m}''_f/\dot{m}''$;

$\dot{m}''_f$ = mass flux of "father" material crossing the control surfaces.

Form suitable for case in which h_S, h_T, f_S and f_T are uniform over the surface considered. In the case described by the sub-title, it is convenient to reduce equations (1) and (2) to the form

$$\mathbf{G}.(\nabla b) - \nabla\{\Gamma(\nabla b)\} = 0 \tag{5}$$

and equations (3) and (4) to the form:

$$\dot{m}'' = \left(\Gamma \frac{\partial b}{\partial y}\right)_S \tag{6}$$

where:

either $$b \equiv \frac{h - h_S}{h_S - h_T} \tag{7}$$

or $$b \equiv \frac{f - f_S}{f_S - f_T}. \tag{8}$$

Variable b is dimensionless and has the significance of a potential, the variation of which over the field has to be determined. Equations (5) and (6) form the centre-piece of the standard formulation of the convective mass transfer problem.

Solutions of the mathematical problem. It is usually convenient to express the solution of equation (5) together with the solution of the relevant equations of motion, in the form

$$\dot{m}'' = g.B \tag{9}$$

$$g/G = F(Re, Pr, B) \tag{10}$$

where

g = mass-transfer conductance, usually varying with location on the surface (lb_m/ft^2h);

$$= \frac{(\Gamma\,[\partial b/\partial y])_S}{B} \tag{12}$$

$$B \equiv b_G - b_S \tag{13}$$

$$= \frac{h_G - h_S}{h_S - h_T} \tag{14}$$

$$= \frac{f_G - f_S}{f_S - f_T} \tag{15}$$

= "driving force" for mass transfer, containing only thermodynamic properties (dimensionless);

G = a reference mass flux (e.g. reference stream velocity times corresponding density) (lb_m/ft^2h), so that

g/G = Stanton number (dimensionless);

Re = reference Reynolds number (dimensionless);

Pr = μ/Γ Prandtl number (dimensionless) (N.B. We could equally well write Sc, Schmidt number, in place of Pr since these quantities are equal in the problems considered here);

$F(\ldots)$ = a function, the form of which depends on the fluid-dynamic boundary conditions, shape of the body, etc.

Equation (9) has a form similar to that of Ohm's Law, albeit for a "non-linear" resistance; for the conductance g depends somewhat on the value of the driving force B, as indicated by equation (10). Of course, if preferred g can be eliminated between equations (9) and (10) without difficulty; or rather it need never be introduced.

Procedure for calculating mass transfer rates. Inspection of the foregoing paragraphs reveals that the problem of predicting a mass transfer rate may be split into two parts:

(i) *Aerodynamic.* Solution of the differential equations, yielding the function $F(\ldots)$ of equation (10). In some circumstances it is more convenient to determine this function by experiment than by mathematical analysis. In either case it is necessary to obtain values of the conductance, g.

(ii) *Thermodynamic.* Evaluation of the driving force B from knowledge of the thermodynamic properties in the G-, S-, and T-states.

It is this separability into aerodynamic and thermodynamic aspects which is brought into emphasis by the use of equation (9). Admittedly, separation is rarely complete; for the particular materials in question exert some influence on g by way of transport-property variations.

2.2. *Graphical representation of thermodynamic properties*

The enthalpy–composition diagram. Bošnjaković [2, 10, 11, 12], Busemann [20] and Spalding [9, 13, 14] have shown how enthalpy–composition diagrams can be used for aiding mass transfer calculations. Although many forms of these diagrams are possible (see [18] for a discussion of the relations between these forms), it is convenient here to consider only the variety in which the ordinate is h and the abscissa is f. Fig. 4 contains a simple example of this

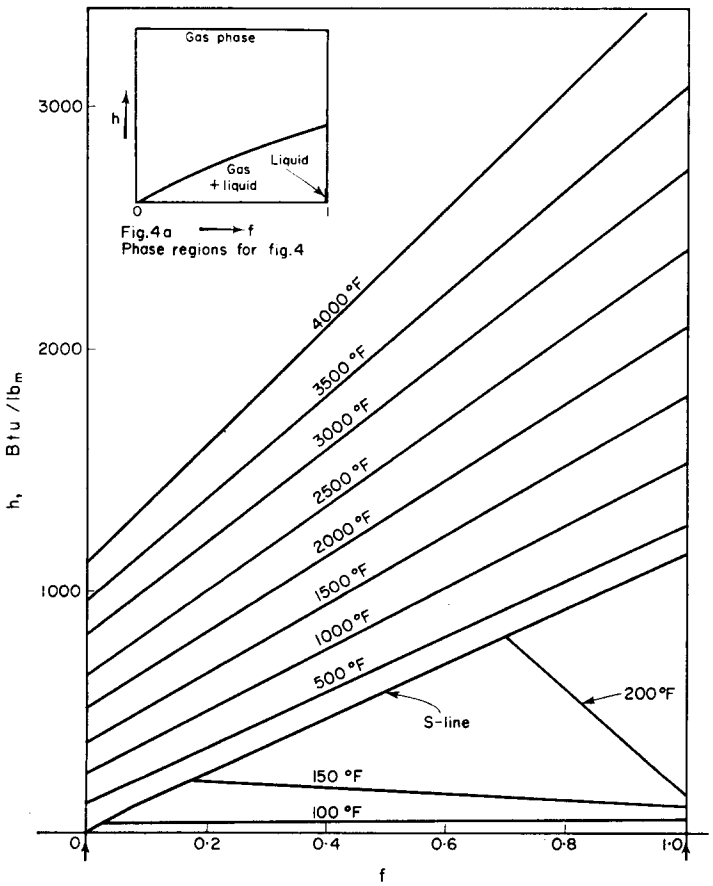

FIG. 4. h-f diagram for H_2O–air mixtures at 1 atm H_2O pressure [9].

U

kind, valid for equilibrium air–steam–water mixtures at 1 atm pressure. Fig. 4 (a) shows which phases prevail in which regions; because no chemical reaction occurs in this case, all constant-temperature lines (isotherms) in the gas-phase region are straight; examples in which these conditions do not obtain will be found below. Because the solubility of air in liquid water is negligible on this scale, the whole liquid region consists of a short portion of the right-hand boundary.

The phase-boundary line. The statements that Fig. 4 is valid for equilibrium and for 1 atm pressure were necessary to explain the position of the curve separating the gas from the gas + liquid regions (marked S-line). In the absence of these statements, all that could be drawn of the *h-f* chart is shown in Fig. 5: the gas-phase isotherms, and the liquid (L) line: but we should not know for how far to the right the gas-phase isotherms were valid. It is possible to draw the gas-phase isotherms and the liquid line without knowing the pressure, since the enthalpies are not appreciably affected by pressure.

Once the position of the S-line is decided for the substances in question, for example by specification of the total pressure and of the existence of equilibrium which together determine f_S for each temperature, the completion of the diagram is easy; the S-line is drawn; the parts of the gas-phase isotherms lying below and to the right of the S-line are erased; and the

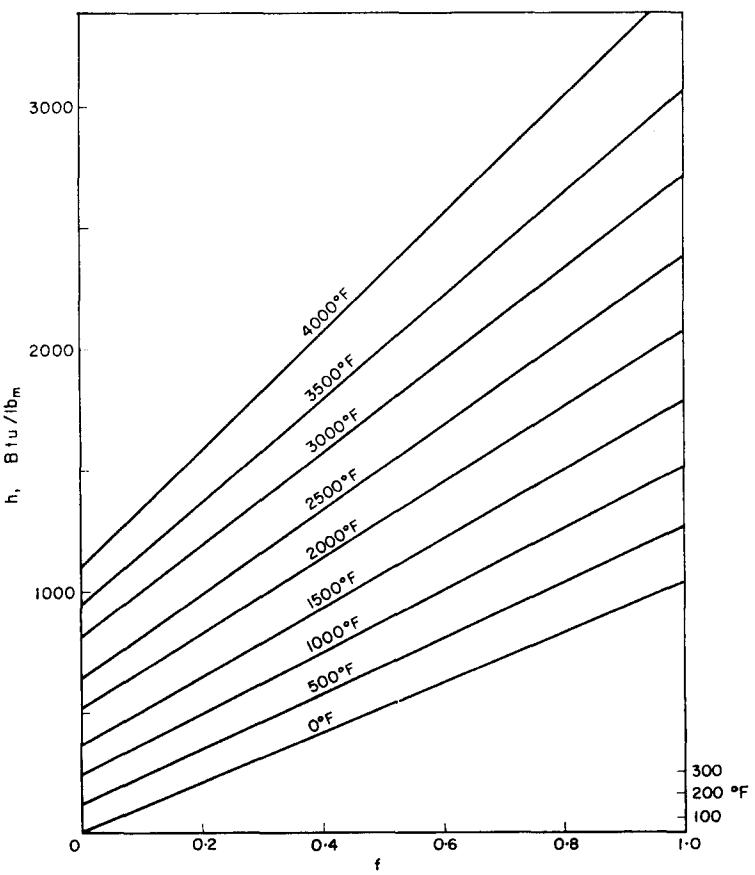

FIG. 5. *h-f* diagram for gaseous H_2O–air mixtures and for liquid H_2O.

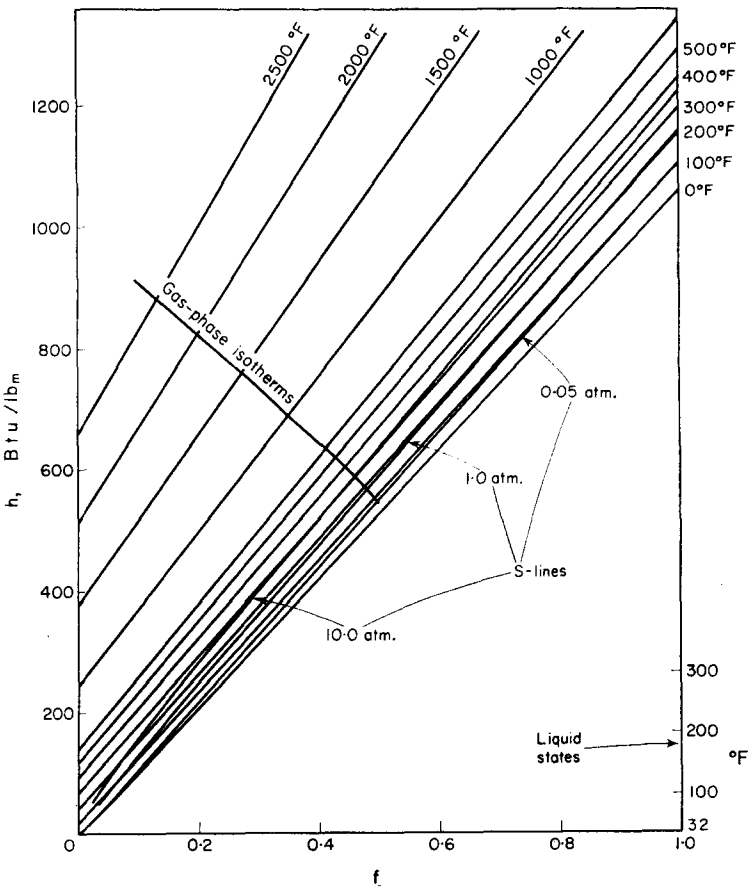

FIG. 6. *h-f* diagram for H_2O–air, showing equilibrium S-lines for three different total pressures.

gas + liquid isotherms are drawn in as straight lines between the corresponding point-pairs of the S- and the L-lines. Fig. 6, which contains for the air–H_2O system the gas-phase isotherms, the L-line, and equilibrium lines for various pressures, thus embodies all the information necessary to provide *h-f* charts for many pressures; for, if a given pressure is selected, the gas-phase isotherms to the right of the appropriate S-line are simply ignored, and the appropriate mixed-phase isotherms are drawn in as just indicated.

However, *the S-line need not be a line representing equilibrium states*; *any* statement concerning the relation between f_S and temperature (or h_S) will suffice to define the S-line on the *h-f* plane. Once this S-line is drawn, the diagram can be completed in the manner explained. Examples of S-lines which do not correspond to equilibrium will be encountered below; they represent the main focus of attention in the present paper.

Graphical representation of the driving force, B. Fig. 7 is a sketch of part of an *h-f* chart showing the S-line and a few isotherms; we need not at present enquire as to whether the gas-states corresponding to points on the S-line are equilibrium states. Points G, S and T are marked on the diagram, corresponding respectively to the states of the main fluid stream, the material in contact with the surface, and the transferred substance, in the standard mass

transfer situation illustrated by Fig. 3; for this to be possible, the *h-f* chart must of course be that for the two parent materials out of which the main-stream and the transferred substance are composed.

Although in all the examples to be considered below the main-stream will be composed entirely of one of the parent substances ($f_G = 0$), Fig. 7 illustrates a rather more general situation ($f_G > 0$), the physical significance of which

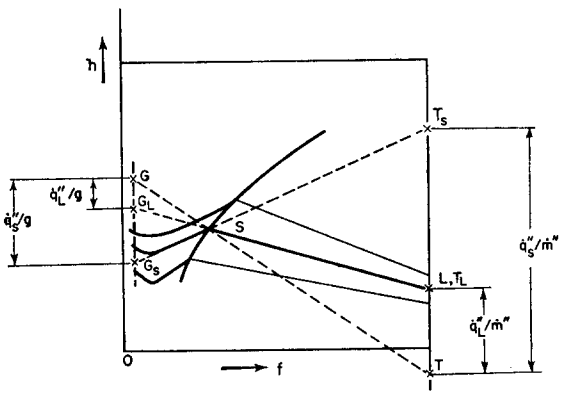

FIG. 7. Representations of states and fluxes on the *h-f* diagram.

should be obvious. The situation represented in Fig. 7 is however non-general in that T is placed on the right-hand boundary ($f_T = 1$); all the examples to be dealt with in the present paper will exhibit this feature, since the transferred substance will always be wholly composed of one of the parent substances in our problems. In general, however, f_T can be either greater or less than unity [8].

G, S and T lie on a straight line. This important result, together with quantitative information concerning the ratio into which S divides GT, follows from consideration of the geometrical significance of equations (13), (14), and (15). We deduce:

$$B = \overline{GS}/\overline{ST} \tag{16}$$

where:

$\overline{GS}$ stands for the length of the line GS, and

$\overline{ST}$ stands for the length of the line ST.

Graphical representation of the heat fluxes. In all the problems to be discussed in the present paper, the transferred substance is the only material present at the control surface L just below the interface. It follows that the L state and the T_L state (defined in Section 2.1) are identical; so the point L can also be marked T_L. We deduce from the definition of h_T that the heat flux through the L control surface is given by:

$$\frac{\dot{q}''_L}{\dot{m}''} = h_{T_L} - h_T \tag{17}$$

and is therefore measured by the vertical distance $\overline{TT}_L$ on Fig. 7.

The state T_S (transferred substance at temperature, phase and state of chemical aggregation at which it crosses the control surface S) can be found on the *h-f* chart by prolonging the pure-phase isotherm through S until it cuts the vertical through T, i.e. the line $f = 1$ in our case. It then follows from the alternative definition of h_T that the heat flux through the S control surface is given by:

$$\frac{\dot{q}''_S}{\dot{m}''} = h_{T_S} - h_T, \tag{18}$$

and so is measured by the vertical distance $\overline{TT}_S$ on Fig. 7.

Also plotted in Fig. 7 are the points G_S and G_L, determined by producing the lines T_S S and T_L S respectively to intersect the vertical through G. The point G_S represents the state of material having the composition (in terms of f) of the main-stream (G) reduced without change of phase to the temperature and state of chemical aggregation prevailing in the fluid adjacent the surface (S-state). The point G_L has a less easily explained physical significance.

These two points are drawn because, by reason of (17), (16), (9), and the geometry of similar triangles, we have:

$$\frac{\dot{q}''_L}{g} = h_G - h_{G_L} \tag{19}$$

which quantity is measured by the vertical height $\overline{G_L G}$; and further, by reason of (18), (16), (9) and the geometry of similar triangles, we have:

$$\frac{\dot{q}''_S}{g} = h_G - h_{G_S} \qquad (20)$$

which quantity is measured by the vertical height $\overline{G_S G}$.

The supply state O, *and the radiative heat flux.* In all the problems to be dealt with in the present paper, the direction of mass transfer is *into* the fluid ($\dot{m}''$ = positive), the material flux through the L surface is wholly convective (composition gradients are absent in the neighbouring phase), and the transferred substance is supplied steadily from a source. Let us designate the state of the transferred substance at the source: "state O". Let us further consider the case in which transverse heat conduction within the neighbouring phase is negligible but in which a radiative heat flux occurs at the surface.

Figure 8 illustrates the situation. The radiant heat flux, $\dot{q}''_{rad}$ (Btu/ft²h), has been darwn as emanating from a region somewhat below the

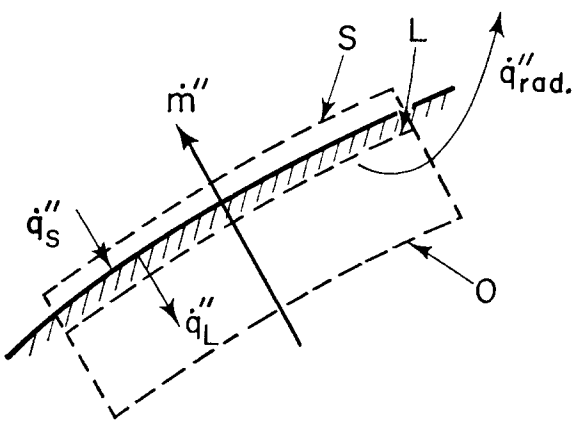

FIG. 8. Control surfaces for derivation of equations (21) and (22).

L-surface rather than from the interface itself; this is a mathematical artifice without physical importance. There are no relevant heat or mass fluxes other than those shown on the diagram.

Application of the steady-flow energy equation to the control volume bounded by the O and L planes in Fig. 8 yields the result:

$$\frac{\dot{q}''_L}{\dot{m}''} = \frac{\dot{q}''_{rad}}{\dot{m}''} = h_{T_L} - h_O \qquad (21)$$

where of course h_O denotes the enthalpy of the transferred substance in its supply state.

Combination of equations (17) and (21) now yields a relation which should make clear the distinction between the transferred-substance state and the supply state. It is:

$$h_O - h_T = \frac{\dot{q}''_{rad}}{\dot{m}''}. \qquad (22)$$

This equation signifies that the enthalpy of the transferred substance differs from that of the supplied material by an amount which accounts for the heat loss by radiation (or, in general, by other means), suffered by the transferred material before it enters the fluid phase. The difference is measured by the length $\overline{TO}$ on Fig. 7.

Determination of the transferred-substance state. In the problems to be considered in the present paper, it will be usual for the supply state O to be specified; for example, in a missile re-entry problem it is the state of the bulk of the heat-shield material before re-entry begins. However the transferred-substance state, T, enters more directly into the calculations. How is the enthalpy of this state determined?

Normally trial and error will be necessary. An assumption must be made about the T-state, for example that it is identical with the O-state. Then the mass transfer rate, $\dot{m}''$, and the surface temperature, t_S, can be calculated. But, once t_S is known, $\dot{q}''_{rad}$ can be calculated. This leads via equation (22) to the enthalpy of the T-state, in general one which conflicts with the original assumption. Use of this new T-state as the starting-point for a new cycle of calculation, together with further iteration if needed, normally leads quickly to the value of h_T, and the location of T, which satisfies all the data of the problem. This procedure is so straightforward that we shall act below as though the T-state is as easily available as the O-state.

2.3. *The problem of* S-*state determination*

The majority of writers on mass transfer use wholly analytical methods, i.e. they are concerned to find and use algebraic relations between the mass transfer rate, $\dot{m}''$, and other relevant quantities. Section 2.1 of the present paper is typical in this regard, equations (9), (10), *et seq.* being the relations in question.

There are however advantages in coupling the analytical methods with graphical representations of thermodynamic properties, specifically with the aid of the enthalpy–composition diagram. The advantages are:

(i) The diagram enables trends to be detected and relative magnitudes of different effects to be compared with an ease which is otherwise scarcely attainable.

(ii) Graphical representation permits "irregular" thermodynamic properties (e.g. variable specific heats, dissociating mixtures) to be handled as easily as more regular ones, in contrast to analytical formulations which become unwieldy in such circumstances.

(iii) In most practical mass transfer problems, the condition of the fluid adjacent the interface (S-state) is not completely specified in the data; so *two* conserved properties have to be considered (e.g. h and f), and their relation in the S-state taken into account. Since the relation is usually non-linear, this is difficult to do analytically: the graphical solution of the problem by contrast presents no difficulty.

It is advantage (iii) which is most relevant to the theme of the present paper. In the present section, therefore, we describe the graphical procedure of the determination of the S-state and subsequent determination of the mass transfer rate.

Procedure for determining the S-*state.* Let us suppose that we have to determine the rate of mass transfer in a situation in which we have as data; the conductance g, the main-stream state G, the transferred-substance state T, and the thermodynamic properties of the relevant substances, but *not* the temperature of the surface nor the composition of the fluid phase adjacent to it. How do we establish the position of S, and hence the values of the driving force B (via equation (16)) and of the mass transfer rate $\dot{m}''$ (via equation (9))?

The data of the problem determine the positions of the points G and T on the h-f diagram. Presuming that this diagram is equipped, like that of Fig. 7, with an S-line, representing the locus of possible S-states, all that is necessary is to draw the join of G and T to intersect the S-line: the intersection is the point S. The ratio $\overline{GS}/\overline{ST}$ is now obtained from a simple measurement, and the problem is as good as solved.

Discussion. Three points should be noted in connexion with the above procedure. Firstly, the procedure is much simpler than its analytical equivalent which involves the solution of two non-linear simultaneous equations, perhaps by the construction of a graph the use of which is restricted to the particular problem. Secondly, the procedure is unaffected by the nature of the considerations which govern the position of the S-line; the line may represent thermodynamic equilibrium, or its position may embody chemical–kinetic constants. Finally, the procedure is only valid in general when the thermal and material exchange coefficients are equal at all points in the fluid (Lewis numbers equal to unity); graphical procedures valid for more general situations remain to be worked out, although a start has been made [9].

2.4. *Problems soluble by use of an equilibrium* S-*line*

As already mentioned, the problems which have been chiefly discussed in the literature are those in which the S-states can be regarded as in thermodynamic equilibrium. Here we shall merely list some of them and note the conditions under which equilibrium can be held to prevail.

The H_2O–*air system.* This system, which is of great importance in heating and ventilating, drying, steam power plant design, etc., has been considered by many authors [9, 11, 12, 20], always with the assumption that gas states adjacent to the interface were in equilibrium with the liquid phase. This assumption of equilibrium is almost invariably justified in terrestrial problems; the reason will become clear in Section 3.1.

The liquid–hydrocarbon–air system. An enthalpy–composition diagram for this system, which differs in character from the H_2O–air one primarily in the fact that a gas-phase chemical reaction occurs, has been presented by Spalding and Tyler [15]. Once again the assumption was made that the gases adjacent to the liquid surface were in equilibrium with the liquid. It is not likely that this assumption is

appreciably in error under the combustion chamber circumstances for which it is usually desired to make calculations.

An enthalpy–composition chart for the rocket fuels, liquid oxygen and kerosene, has been presented by Spalding [14]. Once again the equilibrium assumption was made.

The carbon–air system. Enthalpy–composition charts for this system have been published by Spalding and Tyler [15], and more extensively by Bosnjakovic [2] who has considered also mixtures with steam as third component. A Spalding–Tyler diagram is reproduced in Fig. 9; it is valid for a pressure of one atmosphere.

In all these diagrams the S-line has been drawn through points corresponding to equilibrium mixtures. However it is quite clear that the assumption that state-point S lies on such a line is only valid when the surface temperature is high (say above 2500°F abs.); for otherwise the chemical reaction rate is insufficient to cope with the oxygen diffusing to the surface. This fact, which has been appreciated at least since the investigations of Tu *et al.* [4], will be subjected to quantitative examination in Section 3.2.

The problem of melting ablation. The rate of material disappearance from the surface of a "heat-shield" which melts as well as vaporizes has been considered by Bethe and Adams [21], on the assumption that equilibrium prevails between the liquid material on one side of the interface and the gaseous material on the other. The way in which such calculations can be aided by means of enthalpy–composition charts has been indicated by the present author [14]. However, it appears likely that many of the materials which come in question for "heat-shields" do not exhibit a true equilibrium at the interface: instead there occurs a so-called "pyrolysis reaction" in which the chemical structure of the material is changed in an irreversible manner. No analyses of this situation appear to be available in the literature; one is provided in Section 3.3 below.

A problem to which the equilibrium assumption is totally inapplicable. In the present section we

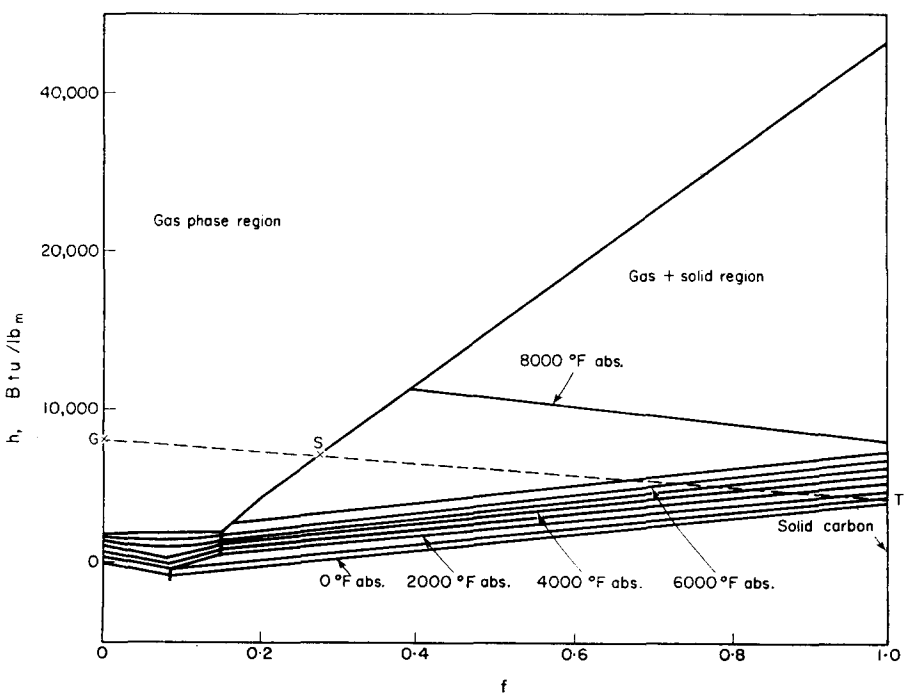

FIG. 9. *h-f* diagram for carbon–air mixtures [15], total pressure = 1 atm.

have listed some of the mixture systems to which the S-equilibrium assumption has been applied, rightly or wrongly, in the past. We conclude this review of past work by mentioning a system for which the equilibrium assumption *cannot* be applied at all. This is the system in which the condensed phase consists of a solid propellant, for example ammonium perchlorate, which reacts exothermically and irreversibly on heating to form a gaseous material of different composition. Since the condensed phase is itself not in thermodynamic equilibrium, no question of equilibrium in the S-state arises. This problem, to which approaches have been made [9, 22], is tackled in Section 3.4 below.

3. MASS TRANSFER PROCESSES IN WHICH THE S-STATE IS NOT IN EQUILIBRIUM

3.1. *Vaporization* and sublimation*

A review of modern knowledge of the kinetics of the phase-changing process in vaporization and sublimation has recently been made by Scala and Vidale [23]. In view of this publication it will suffice here merely to consider the simplest form of this phase change, i.e. that without chemical transformations, and to concentrate on the graphical implications. More concretely, we ask ourselves what changes must be made to the *h-f* diagram of Fig. 4 if the assumption that the S-state is in equilibrium is abandoned.

The kinetics of simple phase change. The net rate at which material changes phase per unit area is the difference between a flux of molecules from the gas phase, which strike the condensed-phase surface and are held on to it, and a flux of molecules from the condensed phase which, because of their above-average energy, break the bonds which hold them and escape. In equilibrium these two fluxes are equal.

The rate of collision of gas molecules with a containing wall is easily calculated from the kinetic theory of gases; it is

$$\overleftarrow{\dot{m}_j} = \frac{\rho_S \, a_{j,\,S} \, m_{j,\,S}}{\sqrt{(2\,\pi\,k_{j,\,S})}} \qquad (23)$$

where $\overleftarrow{\dot{m}_j''}$ = mass rate of collision of molecules of material j with the wall (lb_m/ft^2h);
ρ_S = density of gas mixture in S-state (lb_m/ft^3);
$a_{j,\,S}$ = velocity of sound in a medium of pure j at the temperature of the S-state (ft/h);
$m_{j,\,S}$ = mass fraction of component j for the S-state (—);
$k_{j,\,S}$ = specific heat ratio of material j at the temperature of the S-state (—).

Equation (23) is more usually expressed in terms of molecular weights, the absolute temperature, the pressure, etc.; the above form has been chosen since it is easy to give quantitative significance to the terms in the expression. Thus, if $m_{j,\,S}$ were unity for example, the numerator of the r.h.s. of equation (23) would be equal to the mass flow rate per unit area of a stream of material j flowing through the throat of a convergent–divergent nozzle at the prevailing pressure and temperature: the denominator is a numerical factor of the order of 3. It is clear that collision rates are rather high.

If we assume that the flux of material *from* the condensed phase *to* the gaseous phase, $\overrightarrow{\dot{m}_j''}$, depends only on the surface temperature, and note that at equilibrium it is equal to the fraction α of the colliding molecules which are retained at the surface, we may deduce that the net mass flux of j, $\dot{m}_j''$ is given by

$$\dot{m}_j'' = \overrightarrow{\dot{m}_j''} - \alpha\,\overleftarrow{\dot{m}_j''} = \frac{\alpha\,\rho_S\,a_{j,\,S}}{\sqrt{(2\pi\,k_j)}}\,(m_{j,\,S,\,eq} - m_{j,\,S}) \qquad (24)$$

where $m_{j,\,S,\,eq}$ is the mass fraction of material j which is found in an equilibrium mixture of gas in contact with a condensed-phase surface at the temperature and pressure of the S-state,
α is the proportion of "sticky collisions", assumed to depend only on temperature.

Equation (24) is equivalent of Scala and Vidale's equation (6).

* The necessity for consideration of the kinetics of the phase-change in vaporization was first brought to the author's attention some ten years ago by Dr. S. Traustel of Berlin–Charlottenburg.

Values of α are only known with accuracy for relatively few substances; Scala and Vidale give a review of present knowledge. According to their tabulation, α is approximately equal to unity for water, ice and several solid and liquid materials, but may fall to as low as 10^{-6} for other materials.

Determination of the S-*state.* Equation (24) is not the only relation between the mass transfer rate and the conditions adjacent the interface: we also have that which is implicit in equations (9) and (16). Simultaneous satisfaction of these two relations fixes S and $\dot{m}''$.

We first consider systems in which no chemical reaction occurs in either phase and in which the transferred substance consists entirely of the parent material. Let this material be j. Then f and m_j are identical. Consequently (9) and (15) lead to:

$$\dot{m}'' = \frac{m_{j,\,\mathrm{G}} - m_{j,\,\mathrm{S}}}{m_{j,\,\mathrm{S}} - 1} \cdot g \qquad (25)$$

Eliminating $\dot{m}''$ between (24) and (25), we obtain a relation from which the departure of the S-state from equilibrium can be determined, namely:

$$m_{j,\,\mathrm{S,\,eq}} - m_{j,\,\mathrm{S}} = K_{\mathrm{vap}} \cdot \frac{m_{j,\,\mathrm{G}} - m_{j,\,\mathrm{S}}}{m_{j,\,\mathrm{S}} - 1} \qquad (26)$$

where:

$$K_{\mathrm{vap}} \equiv (g/\rho_{\mathrm{S}}\, a_{j,\,\mathrm{S}})\, \sqrt{(2\,\pi\, k_j/\alpha)}. \qquad (27)$$

Clearly K_{vap} is a dimensionless parameter measuring the "strain" which is placed on the mechanism maintaining equilibrium by the convective phenomena adjacent the surface.

Now equation (26) is a relation between $m_{j,\,\mathrm{S}}$ and t_{S}, i.e. between f_{S} and h_{S}; for m_j and f are identical, h depends only on f and t, and $m_{j,\,\mathrm{S,\,eq}}$ is supposed to be a known function of temperature. Equation (26) therefore defines a curve on the h-f diagram for a fixed value of K_{vap} and of $m_{j,\,\mathrm{G}}$.

The H_2O*-air example.* Fig. 10 shows S-lines drawn on the h-f chart for H_2O–air at one atmosphere pressure. They are valid for various values of K_{vap}, but for a single value of $m_{j,\,\mathrm{G}}$, namely zero.

The line marked $K_{\mathrm{vap}} = 0$ is of course that for equilibrium which has already been encountered in Fig. 4. The lines for positive K_{vap} lie to the left of this line. Negative values of K_{vap} have no physical significance and have been neglected. Although all the lines are somewhat similar in shape to the equilibrium line, those for $K_{\mathrm{vap}} > 0$ turn upwards at the right-hand boundary.

Practical values of K_{vap}. A little reflection concerning the use to which the S-line is put in practical calculations of mass transfer rates (see Section 2.3 above), coupled with inspection of Fig. 10, reveals that departures from equilibrium only assume importance when K_{vap} exceeds the value of 0·1, say. When is this likely to occur in practice?

To answer this question, we first anticipate the result given in Section 4 for the laminar axisymmetric stagnation-point flow. There it is shown that, for small values of B and for a Prandtl number of 0·7, we have:

$$g_{B\to 0} = 0{\cdot}957\, [\mu_{\mathrm{G}}\, \rho_{\mathrm{G}}\, (\mathrm{d}u_{\mathrm{G}}/\mathrm{d}x)]^{1/2}. \qquad (28)$$

Thus, in this case we may write:

$$K_{\mathrm{vap}} \approx \frac{1}{3\alpha} \cdot \frac{[\mu_{\mathrm{G}}\, \rho_{\mathrm{G}}\, (\mathrm{d}u_{\mathrm{G}}/\mathrm{d}x)]^{1/2}}{\rho_{\mathrm{S}}\, a_{\mathrm{S}}} \qquad (29)$$

where the omitted suffix to a_{S} implies that this quantity is evaluated for the transferred substance.

Combining this relation with that of equation (2) for the perpendicular-jet flow, considering the rather extreme case in which the gas emerges from the nozzle at sonic velocity, and noting that $\mu\rho$ is approximately independent of temperature for gases, we find that the condition for $K_{\mathrm{vap}} > 0{\cdot}1$ is:

$$\text{approximately:} \quad \frac{\rho_{\mathrm{S}}\, a_{\mathrm{S}}\, D}{\mu_{\mathrm{S}}} < \frac{10}{\alpha^2}. \qquad (30)$$

Now at 1 atm and 32°F in air, $\rho_{\mathrm{S}} = 0{\cdot}0807$ $\mathrm{lb_m/ft^3}$, $a_{\mathrm{S}} = 3{\cdot}9 \times 10^6$ ft/h, and $\mu_{\mathrm{S}} = 0{\cdot}042$ $\mathrm{lb_m/ft\,h}$; therefore $\rho_{\mathrm{S}}\, a_{\mathrm{S}}/\mu_{\mathrm{S}} = 7{\cdot}5 \times 10^7\ \mathrm{ft^{-1}}$. It follows that the jet diameter must be less than $1{\cdot}3 \times 10^{-8}$ ft if α is of the order of unity and the vaporization kinetics are to be significant. Even if the pressure is reduced to 10^{-3} atm, an extremely low value, the required jet diameter is very much smaller than normally encountered.

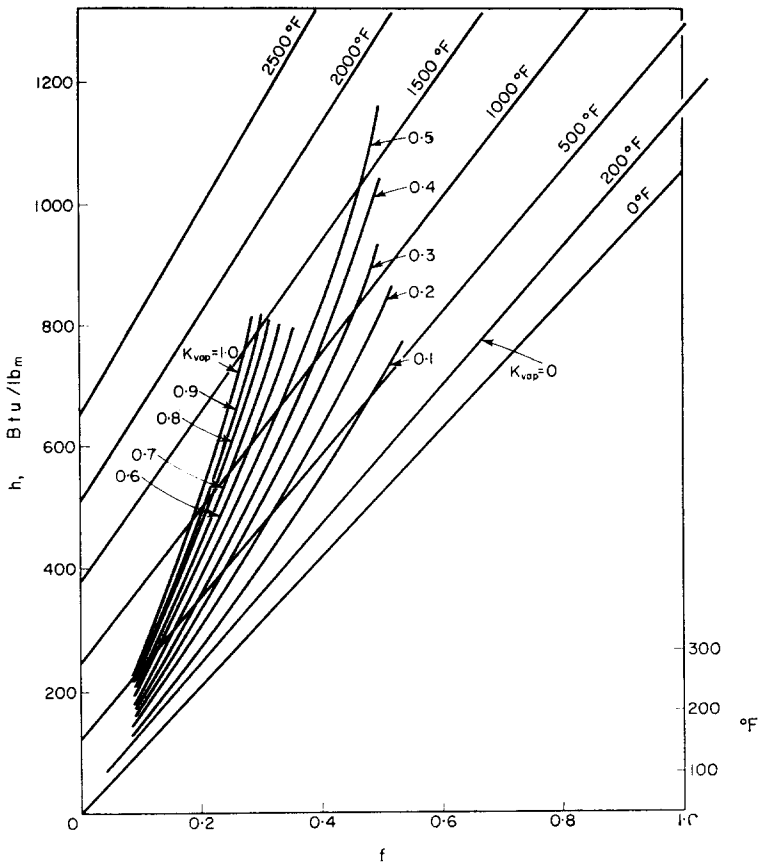

FIG. 10. *h-f* diagram for H_2O–air mixtures at 1 atm, showing S-lines for various K_{vap}.

On looking into this situation somewhat more closely, it appears that, if the coefficient α is of the order of unity, the vaporization kinetics only become important when the apparatus dimensions approach those of the molecular mean free path in the gaseous medium. This situation is rare; indeed, when it does occur, the conventional means of calculating mass-transfer conductances have to be reviewed in any case.

More general cases. If the vaporizing material reacts chemically with the surroundings, we can no longer equate m_j and f. Nevertheless there does exist a relation between these quantities, determined by the stoichiometry of the chemical reaction. By its aid one can proceed as in the above simple example and calculate a relation between f_S and h_S for prescribed G-state and K_{vap} values, and so plot a family of S-lines on the *h-f* chart.

However, the conclusion reached in the H_2O–air example applies to these more general cases also; it is only when α is very much less than unity, or when the molecular mean free path is not small compared with the apparatus dimension, that there is ever any need in practice to consider any S-line but that for $K_{vap} = 0$.

3.2. *The combustion of a solid fuel in an oxidant stream*

The main conclusion which may be derived from Section 3.1 is that departures of the S-state from the equilibrium line can seldom be

important; this will not be true of the situation now to be discussed however.

Kinetics of the heterogeneous reaction. For simplicity, we shall first imagine that the fuel is wholly non-volatile and that the gaseous oxidant reacts with it at the surface to form a unique product by way of a chemical reaction which can be represented as:

Fuel (solid) + oxidant (gas) → product (gas)

1 lb_m r lb_m $1 + r$ lb_m.

The simplest law which we can expect the rate of chemical reaction to obey is then as follows:

$$\dot{m}'' = \frac{\overleftarrow{\dot{m}''_{ox}}}{r} \cdot \exp(-E/\mathscr{R}T_S) \qquad (31)$$

where $\overleftarrow{\dot{m}''_{ox}}$ = rate of collision of oxidant molecules with the surface (lb_m/ft^2h) to be calculated from equation (23);

E = activation energy of the chemical reaction (Btu/lb mole);

$\mathscr{R}$ = universal gas constant = 1·98 (Btu/lb mole °F abs.);

T_S = absolute temperature prevailing at the surface (°F abs.);

r = stoichiometric ratio (lb_m oxidant/lb_m fuel).

Here the "Arrhenius factor", $\exp(-E/\mathscr{R}T_S)$, accounts for the fact that only collisions with a sufficient energy of impact will suffice to loose a fuel molecule from its bonds and cause it to enter a chemical reaction.

More general relations than (31) may involve a multiplying constant which accounts for the small-scale texture of the surface and which possibly shows secondary dependences on temperature, pressure and oxidant concentration.

Determination of the S-*state.* It has been shown elsewhere [1, 5, 8], that the mass transfer driving force appropriate to the present situation is:

$$B = \frac{m_{ox,G}/r - m_{ox,S}/r}{1 + m_{ox,S}/r}. \qquad (32)$$

Combining (32), (9), (23) and (31) therefore, we obtain an equation from which the oxygen concentration at the surface may be established. It is:

$$\frac{m_{ox,S}}{r} = K_{ox} \cdot \frac{m_{ox,G} - m_{ox,S}}{r + m_{ox,S}} \cdot \exp(+E/\mathscr{R}T_S) \qquad (33)$$

where

$$K_{ox} \equiv \frac{g\sqrt{(2\pi k_{ox,S})}}{\rho_S a_{ox,S}}. \qquad (34)$$

Now equation (33) defines a family of lines on the enthalpy–composition chart for fuel and oxidant mixtures, with K_{ox} and $m_{ox,G}$ as parameters; for to every pair of values of $m_{ox,S}$ and T_S there corresponds a point on the diagram.* Thus a family of S-lines can be drawn on the diagram with K_{ox} as parameter if $m_{ox,G}$ is held fixed; clearly, if K_{ox} is very small, the S-line coincides with that for thermodynamic equilibrium; finite values of K_{ox} lead to finite values $m_{ox,S}$ and so to reduced values of the driving force.

S-*lines on the h-f chart.* The value of the quantity E is such that $\exp(-E/\mathscr{R}T_S)$ varies steeply with temperature in the range of practical interest. For example, if E = 30,000 Btu/lb mole, and T_S = 1500°F abs., a 1 per cent increase in T_S brings about a 10 per cent increase in $\exp(-E/\mathscr{R}T_S)$. As a consequence, the constant-K_{ox} lines on an enthalpy–composition chart may look like those sketched in Fig. 11; at high-to-moderate temperatures they hug the line $K_{ox} = 0$; at lower temperatures they move rapidly across to the left-hand boundary.

In passing, it may be noted that the shape of the S-lines ensures that, with the main-stream and transferred-substance states as indicated by G and T in the diagram, there are in general *three* possible S-points for each value of K_{ox}. If K_{ox} increases above a limiting value, however, two of the intersections become imaginary, leaving only the one close to the point G. These

* For example m_{ox} is uniquely related to f by the stoichiometric relation:

$$f < \frac{m_{ox,G}}{r + m_{ox,G}}: \quad f = \frac{m_{ox,G} - m_{ox}}{r + m_{ox,G}} \qquad (34a)$$

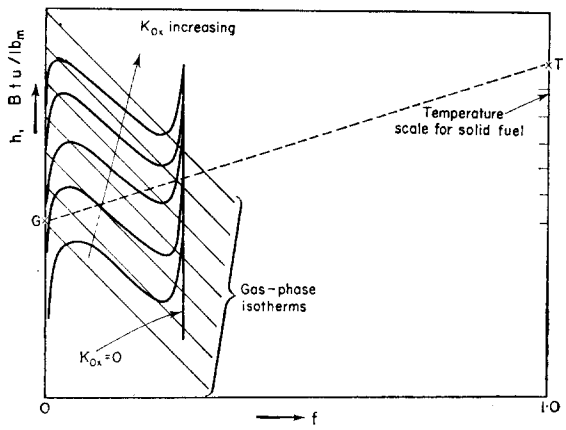

FIG. 11. Sketch of *h-f* diagram for hypothetical non-volatile solid fuel forming single oxide, showing a family of S-lines with K_{ox} as parameter.

facts correspond to the well-known phenomenon of the extinction of a solid-fuel combustion resulting from excessive mass transfer; the phenomenon has been discussed by many authors (see [24] for a literature review).

Relevance to the combustion of carbon in air. The process of the combustion of carbon in air is somewhat more complicated than the one just discussed, a fact which is evidenced by comparison of the shapes of the equilibrium S-lines in Fig. 9 on the one hand and Fig. 11 on the other. The differences between carbon and our model are of two kinds:

(i) carbon can form two different oxides, CO and CO_2, the first being the equilibrium product at high temperatures, the second that at low temperatures;

(ii) carbon sublimes if the temperature is raised to a high enough value ($> 7000°F$ abs. at 1 atm pressure).

Both these differences introduce complications of the same kind: chemical reaction now has to be considered in the gas phase. Thus if the surface temperature is low, composition distributions in the boundary layer may be as shown in Fig. 12 (a), with gas-phase combustion of carbon monoxide and with the heterogeneous reaction occurring between carbon and carbon dioxide; whereas if the surface temperature is very high, as illustrated in Fig. 12 (b), possibly on heterogeneous reaction occurs at all.

Order-of-magnitude considerations. A rigorous treatment of the situation just indicated is possible, but requires a paper all to itself. Here we shall be content to show (i) that at the high temperatures at which sublimation is important it is probably sufficient to assume that equilibrium prevails; (ii) that if radiation is absent it suffices to regard carbon monoxide as the main combustion product at the surface.

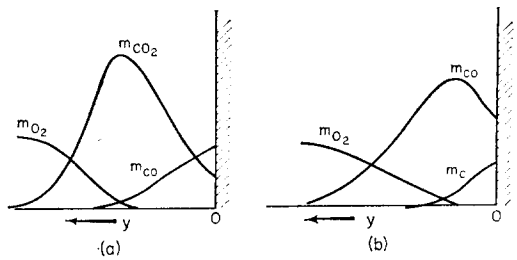

FIG. 12. Possible gas-composition distributions adjacent burning carbon surface: (a) moderate surface temperature, (b) very high surface temperature.

Values of the activation energy E of carbon reacting heterogeneously with oxygen and with carbon dioxide can be found in the combustion literature. Papers which might form the starting points for a thorough survey are referenced [6, 7, 25]. Quoted values of E range from 36,000 to 125,000 Btu/lb mole, the lower values being more common for the reaction with oxygen. Let us take $E = 45{,}000$ Btu/lb mole as a representative value.

Now in practice K_{ox} may have values around 10^{-3}, as may be seen by noting that Stanton numbers are commonly around 3×10^{-3}, Mach numbers around 0·1 and $\sqrt{(2\pi k_{ox,s})}$ around 3. For departures from equilibrium to be appreciable therefore, $\exp(E/\mathscr{R}T_S)$ must exceed 10^2. But at $T_S = 7000°F$ abs. with $E = 45{,}000$ Btu/lb mole; $\exp(E/\mathscr{R}T_S)$ is no more than 25. It follows that by the time that the surface has reached the temperature at which sublimation occurs (at 1 atm), the chemical reaction rate is sufficiently fast practically to ensure equilibrium at the surface. We conclude that the upper

sloping portion of the equilibrium S-line shown in Fig. 9 can usually be safely used.

Further inspection of Fig. 9 reveals that, in the absence of radiation loss (states T and O identical) the equilibrium surface temperature is above 2000°F abs. and the equilibrium composition corresponds to combustion to carbon monoxide ($f_S = 0{\cdot}148$). Indeed, if this were not so, $\exp(E/\mathscr{R}T_S)$ would be so far in excess of 10^4 that combustion could hardly take place at an appreciable rate. It therefore appears as though the burning of a carbon heat-shield, for example, can be fitted into the framework constructed for the model which was introduced at the beginning of Section 3.2, at least provided that information is available about the diffusion flame which forms.

Although it is not intended to deal fully in this paper with the diffusion flame shown in Fig. 12 (a), the following remarks should be made:

(i) If the rate of the gas-phase reaction between carbon monoxide and oxygen is sufficiently high, the flame will exist and will prevent direct access of oxygen to the carbon surface.

(ii) If the rate of this reaction is insufficiently high, the diffusion flame will not exist; oxygen then reaches the carbon surface.

(iii) At least when the gas-stream temperature is low, the transition from the first state to the second is a sudden one, occurring at a critical value of a dimensionless quantity composed of a volumetric reaction rate constant times Γ divided by the square of the mass transfer rate through the flame region. This extinction phenomenon has been considered theoretically by Zeldovich [26] and by Spalding [27].

(iv) The presence or absence of the diffusion flame makes no difference to the *equilibrium* S-line, but it does affect the positions of the S-lines for finite K-values; for the activation energy, for example, is different according to whether the carbon reacts with carbon dioxide or with oxygen.

(v) If the diffusion flame *is* present, so that carbon dioxide is the oxidant, the relation of m_{CO_2} to f is as follows:

$$\frac{m_{O_2,\,G}}{(32/12) + m_{O_2,\,G}} \leqslant f \leqslant \frac{m_{O_2,\,G}}{(16/12) + m_{O_2,\,G}} :$$

$$f = \frac{m_{O_2,\,G} - (16/44)\, m_{CO_2}}{m_{O_2,\,G} + (10/12)}. \quad (34b)$$

Concluding remarks on carbon combustion. The foregoing study of the model solid fuel should have made clear how the kinetic constants of the heterogeneous reaction(s) influence the position of the S-line which must be drawn on the enthalpy–composition diagram. It should also by now be apparent that the more complex kinetics of the carbon–air system will lead to a corresponding family of S-lines by a path which is somewhat more tedious to compute, since gas-phase kinetics demand consideration, but which is not essentially different. Are we in a position to carry out the latter task?

While a complete survey of the literature is necessary before a negative answer can be given with certainty, it appears to the present author that the published kinetic constants have been determined under circumstances which are sufficiently different from those of the laminar stagnation-point flow, for example, to render reliance on the data unwise; for example the actual surface area of the carbon, taking into account internal pores, has often been uncertain in past investigations. In these circumstances it appears likely that an *experimental* determination of the location of the S-lines on the h-f diagram is desirable for each new sort of carbon which comes in question, for example, as a heat-shield material.

A suitable experimental arrangement is that shown in Fig. 2. Suitable measurements are: burning rate, surface temperature, and extinction condition. The existence of the theoretical framework of the present paper renders unnecessary provision in the experiment of the precise conditions of the "heat-shield" operation. Thus one may use pure oxygen in the gas stream instead of air, and supply heat to the carbon electrically instead of letting it be extracted by radiation. In this way it may well be possible to make simple but relevant laboratory studies of a

material which is ultimately to be used in the outer layers of the earth's atmosphere.

3.3. *Surface pyrolysis*

In Section 3.2, one of the components of the gas stream reacts chemically with the material of the condensed phase. There are however important processes in which the effect of the gas stream is simply to raise the temperature of the surface, the material of which then decomposes, either exothermically or endothermically. Although only a few materials of this type have been studied, for example ammonium chloride and Plexiglas 1A [28], there seems to be little doubt that the class of materials which pyrolyse is a large one. It is probable that materials used for heat-shields of the "melting-ablation" type fall into this class.

The kinetics of pyrolysis. The studies of Schultz and Dekker [28], as well as theoretical considerations, lead to the conclusion that the pyrolysis reaction obeys the relation:

$$\dot{m}'' = Z_{\text{pyr}} \cdot \exp(-E/\mathscr{R}\, T_S) \qquad (35)$$

where Z_{pyr} is a constant for the condensed phase material depending slightly on surface temperature but almost independent of pressure and of gas-phase composition ($\text{lb}_\text{m}/\text{ft}^2\text{h}$).

We see that this equation fits into the same family as that to which the kinetic equations for simple phase-change and solid-fuel-combustion belong, namely:

$$\dot{m}'' = F(f_S, h_S) \qquad (36)$$

although it has a particularly simple form.

Determination of the S-*lines.* Eliminating $\dot{m}''$ between equations (35), (9) and, say, (15), we obtain a relation which defines a family of S-lines. It is:

$$\frac{1-f_S}{f_S-f_G} = K_{\text{pyr}} \exp(E/\mathscr{R}\, T_S) \qquad (37)$$

where

$$K_{\text{pyr}} \equiv g/Z_{\text{pyr}}. \qquad (38)$$

Here f_T has been placed equal to unity for reasons explained earlier.

Figure 13(a) is a sketch of the *h-f* diagram for mixtures of a pyrolysing solid material with a gas with which it does not react chemically. Pure-phase isotherms are shown, together with S-lines drawn for a single value of f_G (namely

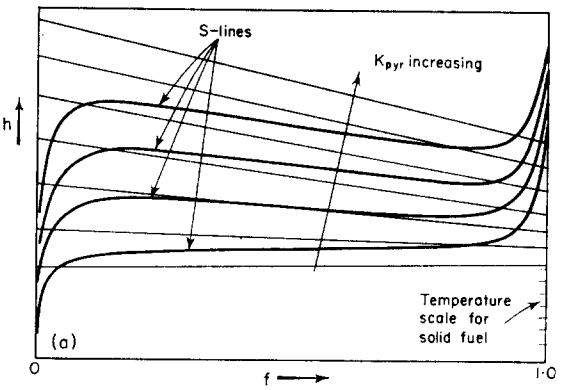

FIG. 13(a). Sketch of *h-f* diagram for a pyrolysing solid which does not react chemically with the material of the gas stream, showing S-lines for various K_{pyr}.

zero) and various values of K_{pyr}. It is seen that as K_{pyr} increases, the S-line moves up and to the left, signifying that the mass transfer driving force, for fixed G- and T-states, must decrease.

Figure 13(b) sketches the complete *h-f* diagram, derived from Fig. 13(a), for a *particular* value of K_{pyr}. The diagram has been drawn for a substance which exhibits a liquid phase for comparison with the equilibrium treatment of

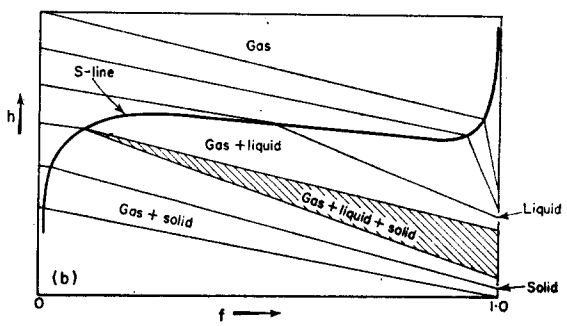

FIG. 13(b). Sketch of *h-f* diagram for a pyrolysing material exhibiting both solid and liquid phases. Diagram is drawn for a particular value of K_{pyr}. No gas-phase reaction is supposed to occur.

melting ablation given by Spalding [8, 14, 18]. As explained in the latter reference, the actual position of the state-point S in any particular problem is governed by the liquid viscosity–temperature relation as well as by the G-state; it is hoped to return to this subject in a later publication.

Discussion. It is clear that the phase-changing mechanism considered in the present section has not introduced any essential novelty: it can be handled by the same procedures as the other mechanisms, merely requiring somewhat differently shaped curves.

It should also be apparent that we can deal in the same way with materials for which the pyrolysis products themselves react with the gases in the main-stream; this situation has elements in common with the carbon–air system where the oxide produced at the surface (CO) can react elsewhere in the boundary layer to form carbon dioxide. Provided that the chemical reaction-rate constants in the gas phase can be taken as very large, no new problem arises.

Another generalization of the situation which it would be easy to handle is that in which the phase-changing reaction was *reversible*. Such a reaction would exhibit an equilibrium condition at values of f less than unity; correspondingly an equilibrium ($K_{\text{pyr}} = 0$) line would appear in the family of S-lines sketched in Fig. 13(a).

3.4. *Combustion of a solid oxidant in a stream of fuel gas*

Nature of the problem. We now consider a more complex class of materials: the solid propellants. Those of the composite variety consist of crystals of solid oxidant, for example ammonium perchlorate, embedded in a matrix of solid hydrocarbon material. It is probable that in an important part of the combustion process the oxidant crystals are suspended in a stream of fuel vapour and that chemical reactions occur at the oxidant surface and in the gas regions around it (Fig. 14a).

Often the oxidant is capable of sustaining a steady combustion in the complete absence of a fuel; this is true of ammonium perchlorate, for example. Even then it is believed that at least two chemical reactions occur, corresponding to three possible states of chemical aggregation of the oxidant. The latter are:

(1) Initial state, solid phase (e.g. $NH_4\ ClO_4$)
(2) Intermediate state, gaseous phase (e.g. $NH_3 + HClO_4$)
(3) Reacted state, gaseous phase (e.g. $NO + HCl + \frac{3}{2} H_2O + \frac{3}{4} O_2$).

We shall refer to the states as: oxidant$_1$, oxidant$_2$, and oxidant$_3$.

The reactions are therefore:

(1) → (2); this causes a phase change and is a surface pyrolysis reaction of the type discussed in Section 3.3.
(2) → (3); this is a gas-phase reaction and occurs in a deflagration wave.

The reaction (2) → (3) is always exothermic,

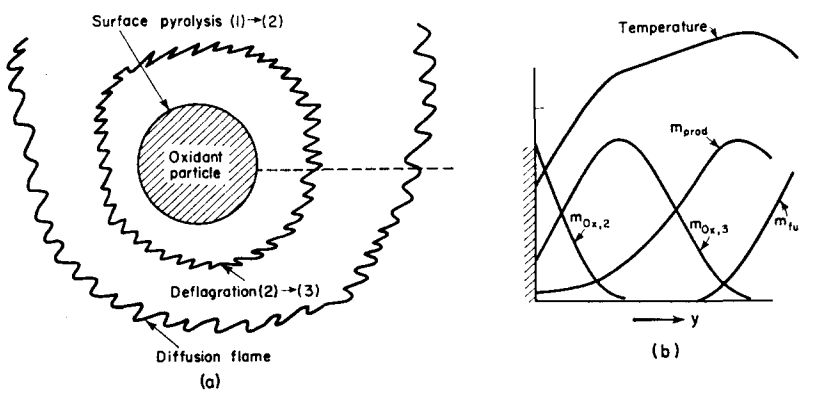

FIG. 14 Illustrating the combustion of an oxidant particle in a fuel–gas atmosphere.

and the reaction (1) → (2) is sometimes exothermic, though not, as it happens, for ammonium perchlorate. The theory of the combustion of propellants of this kind *in the absence of fuel* has been treated by Spalding [19] and by Rosen [29]. When the above reactions occur in the neighbourhood of a source of fuel gas, at least one further chemical reaction occurs: that between oxidant$_3$ and fuel to form a final product. The possibility of this is revealed by inspection of the composition of the third stage of ammonium perchlorate above.*

Figure 14 (a) sketches the situation which may arise when an oxidant particle is suspended in a fuel-gas stream. Three regions of chemical reaction may be discerned: the particle surface when the (1) → (2) pyrolysis occurs; a deflagration region where the (2) → (3) reaction occurs; and a diffusion flame region where oxidant$_3$ combines with fuel gas. Fig. 14 (b) sketches corresponding temperature and composition profiles along the broken line shown in Fig. 14 (a).

The enthalpy–composition diagram. In earlier diagrams for mixtures in which gas-phase reaction occurs, e.g. Fig. 9, we have tacitly drawn the gas-phase isotherms which are valid for gas-phase equilibrium. In this way we have deferred to another place the investigation of the influence of the kinetics of the diffusion flame and its interaction with the mass transfer process.

If we continue this practice in the present problem, the gas-phase isotherms will appear as in Fig. 15, with the oxidant as the "father-substance". Here the lines which slope upward on the left represent mixtures of fuel and final-product gases, while those sloping upward to the right represent mixtures of final-product with oxidant$_3$; the condensed-phase is represented by the temperature scale marked "oxidant$_1$" on the right-hand border. What has happended to oxidant$_2$? The answer is that if gas-phase kinetics are very fast, as will always occur at high pressures, oxidant$_2$ does not appear anywhere in finite concentration.

* That composition is given as an example of how the atoms *might* re-arrange themselves; in reality more compounds will be found in the third stage.

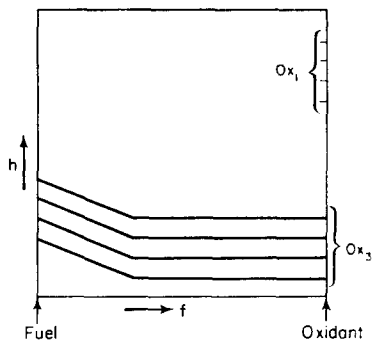

FIG. 15. *h-f* diagram for fuel–oxidant gas-phase mixtures if all gas-phase reactions are very fast.

Alternative diagrams. We could however make the assumption that the kinetics of the diffusion flame are very fast, while those of the (2) → (3) reaction are very slow. In this case material (3) will not appear in finite concentration, the diffusion-flame reaction takes place between oxidant (2) and fuel, and the *h-f* chart will look like Fig. 16. Alternatively we could

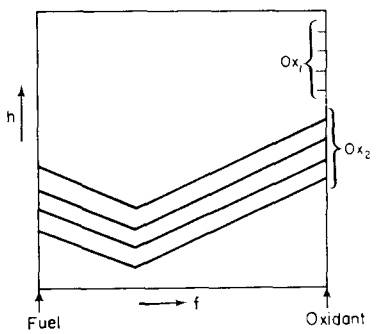

FIG. 16. *h-f* diagram for fuel–oxidant gas-phase mixtures if the diffusion flame reaction is fast but the (2) → (3) deflagration is slow. The (1) → (2) reaction is exothermic in the case shown.

consider the situation in which the kinetics of the (2) → (3) flame are fast, whereas those of the diffusion flame are very slow. This would lead to an *h-f* chart such as is shown in Fig. 17.

Yet another extreme assumption is that *all* gas-phase kinetics are slow. Then neither oxidant$_3$ nor final products appear in finite concentration, neither deflagration nor diffusion

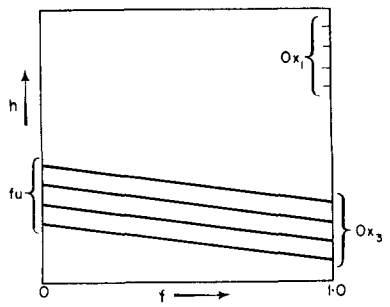

FIG. 17. *h-f* diagram for fuel–oxidant gas mixtures if diffusion–flame reactions are slow but deflagration reactions fast.

flame occurs, and the enthalpy–composition diagram takes the form shown in Fig. 18.

The first of these four diagrams (Fig. 15) can be expected to be valid for high gas pressures, for then chemical reaction rates per unit volume are fast. The last of the diagrams (Fig. 18) correspondingly can be expected to hold for low gas pressures. The charts of Figs. 16 and 17 represent other extreme situations which may sometimes be encountered.

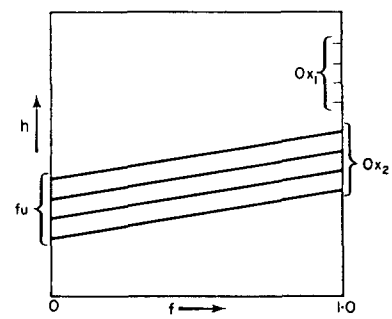

FIG. 18. *h-f* diagram for fuel–oxidant gas mixtures if all gas-phase reactions are slow.

Calculation of mass transfer rate under extreme circumstances. If any of the above extreme situations is known to hold, the calculation of the mass transfer (burning) rate can be easily carried out in a manner similar to that of the above sections. In each case a pyrolysis law is required such as that of equation (35); if Z_{pyr} depends upon the composition of the material adjacent the surface (S-state), this dependence must be known. Then S-lines are plotted on the appropriate *h-f* chart in the same way as before, with K_{pyr} as parameter. The driving force B, and thereafter the mass transfer rate $\dot{m}''$, can then be found for a given pair of G- and T-states by the graphical technique described in Section 2.

Calculation of the mass transfer rate with finite (2) → (3) *kinetics.* We shall now consider how the mass transfer rate can be calculated when none of the above extreme situations prevails. This is a more difficult problem than any that have been tackled above, and requires an excursion into the theory of flame propagation. Fortunately a recent paper by Adler and Spalding [22] has dealt with the flame–theoretical aspects of the problem: it will suffice here to cite and interpret their result. Attention will be focussed on the (2) → (3) flame; as in the case of carbon combustion, we shall simply suppose that knowledge is available about the existence or otherwise of the diffusion flame.

Let us suppose that the G- and T-states are fixed. This means that the line GT on the *h-f* diagram is fixed on which the point S, and indeed all other gas-phase state-points appropriate to the mixing field, must lie. Of course, since none of the extreme situations prevails, we are uncertain as to the location of all the isotherms on the *h-f* diagram.

Nevertheless let us consider the gas states lying on the line GT, and sketch the expected temperature distribution using f as the abscissa; this is shown in Fig. 19. (*N.B.* If an *h-f* diagram

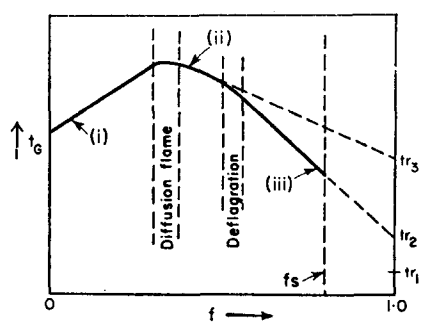

FIG. 19. Temperature near solid–oxidant surface, plotted against f.

is regarded as a contour map with temperature corresponding to altitude, Fig. 19 can be regarded as a "section" through the "hill" represented on the h-f diagram). The temperature distribution exhibits the following features:

(i) An approximately straight* portion rising from the point corresponding to the G-state ($f = 0$, $t = t_G$) to the region marked "diffusion flame".

(ii) A second approximately straight portion between the "diffusion-flame" and "(2) → (3) flame" regions. Along this line the gases are approximately in equilibrium: no oxidant$_2$ is present.

(iii) A third approximately straight line running from the region of the (2) → (3) flame towards a point of termination corresponding to the S-state. In this region the gases are not in equilibrium, but the temperature is too low for oxidant$_2$ to decompose at an appreciable rate.

(iv) Along the right-hand boundary, points marked $t_{T,1}$, $t_{T,2}$, $t_{T,3}$ corresponding to the temperatures of the transferred substance T measured on the scales appropriate to oxidant$_1$, oxidant$_2$ and oxidant$_3$ respectively.

Figure 19 is a sketch: most of it could however be drawn to scale from thermodynamic information alone. The two main features which require extra-thermodynamic knowledge are: the slope of the line passing (after extrapolation) through $f = 1$, $t = t_{T_2}$, which is mentioned in (iii) above; and the point at which this line terminates, i.e. the S-state. We now consider how these features may be determined.

Facts about flame propagation in an enthalpy gradient. It is evident from Fig. 19 that the (2) → (3) deflagration differs from that considered in most flame-propagation studies through being embedded in a region of varying enthalpy; thus, downstream of the reaction zone the temperature has a rising trend instead of becoming uniform. It is precisely the effect of this non-uniformity which has been studied by Adler and Spalding [22]. These authors find that the effect can be characterized, for a given kinetic scheme, by a relation between a dimensionless burning rate:

$$\dot{m}''_{(2)\to(3)}/\dot{m}''_{(2)\to(3),\ T,\ \mathrm{ad}}$$

and a dimensionless gradient parameter η which, in terms appropriate to the present problem, equals the slope of the line marked (ii) in Fig. 19 divided by that of the line marked (iii).† Fig. 20 shows an example of such a relation valid

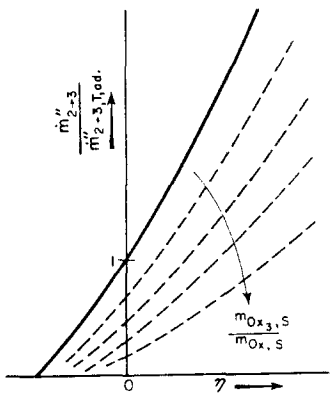

FIG. 20. Influence of enthalpy gradient and surface condition on the (2) → (3) deflagration rate for fixed T-state.

for a first-order reaction and a particular activation energy. Of course the quantity $\dot{m}''_{(2)\to(3)\ T,\ \mathrm{ad}}$ is the mass flow rate in an adiabatic deflagration in which gaseous oxidant$_2$ with enthalpy h_T turns into gaseous oxidant$_3$ with the same enthalpy; this mass flux depends upon pressure as well as upon h_T.

Adler and Spalding were primarily concerned with gaseous flames and therefore paid no attention to the fact that, in solid-propellant combustion, the gaseous deflagration rate is reduced, for fixed enthalpy, by increasing surface temperature; this effect is explained quantitatively and in some detail, by Spalding [19]. If the two effects are taken into account, the relation of Fig. 20 becomes a family of curves,

* If specific heats were temperature independent, the curve would be straight in all regions where chemical reaction was not occurring.

† Adler and Spalding considered constant specific heats; we shall have to do the same here. They used the symbol E for the quantity denoted by η in the present paper.

the parameter being $m_{ox,\,3,\,S}/m_{ox,\,S}$, the ratio of the concentration of oxidant at the surface to the total concentration of oxidant. When this ratio is small, the Adler–Spalding relation holds; when the ratio is large, the burning rate is reduced, falling finally to zero as the ratio tends to unity.

The quantities appearing in Fig. 20 are highly relevant to the two unknown features of Fig. 19: for η is a gradient ratio, knowledge of which enables the line (iii) to be drawn; while the ratio $m_{ox,\,3,\,S}/m_{ox,\,S}$ varies linearly between zero at $f = 1$ and unity at the join of lines (ii) and (iii).

The three simultaneous requirements. It is now evident that the steady-state condition which prevails at the surface and in the boundary-layer must be such as to satisfy three separate and simultaneous requirements. The first accounts for the happenings within the gaseous deflagration, and is portrayed in Fig. 20; it can be written as:

$$\frac{\dot{m}''_{(2)\to(3)}}{\dot{m}''_{(2)\to(3),\,T,\,ad}} = F\left(\eta, \frac{m_{ox,\,3,\,S}}{m_{ox,\,S}}\right). \quad (39)$$

The second accounts for the surface pyrolysis law and can be written:

$$\frac{\dot{m}''_{(1)\to(2)}}{\dot{m}''_{(2)\to(3),\,T,\,ad}} = \frac{Z_{pyr}}{\dot{m}''_{(2)\to(3),\,T,\,ad}} F(t_S). \quad (40)$$

The third accounts for the transport processes in the boundary layer, and can be written:

$$\frac{\dot{m}''}{\dot{m}''_{(2)\to(3),\,T,\,ad}} = \frac{g_{B\to O}}{\dot{m}''_{(2)\to(3),\,T,\,ad}} \cdot F\left(\frac{f_S}{1 - f_S}\right). \quad (41)$$

Here $F(\ldots)$ in each case stands for "a known function of . . .", although of course the function is different for each equation. It will be noted that the mass flux appearing in the denominator of the left hand side has been made the same for each equation

The problem of determining the mass transfer rate is the same as that of solving equations (39), (40) and (41) simultaneously. Firstly however we need to consider the relationships between the quantities $\dot{m}''$, $\dot{m}''_{(1)\to(2)}$ and $\dot{m}''_{(2)\to(3)}$. The first two of these quantities are equal; for they both refer to the mass rate of material entering the gas phase per unit surface area. The last quantity may however be different; for it refers to the mass flux across a different plane. We shall however restrict consideration to the simplest case, namely that in which all three mass fluxes are equal; this occurs in practice if the deflagration $(2) \to (3)$ is very close to the surface, i.e. if the deflagration thickness is much less than the boundary-layer thickness. Although it is possible to deal with the case of unequal mass fluxes, calculation of the ratio between them requires a closer look at a particular flow pattern than is appropriate to the present paper.

Determination of the mass transfer rate. We shall describe the operations which must be performed in order to determine $\dot{m}''$ when the following data are available: values of $\dot{m}''_{(2)\to(3),\,T,\,ad}$, Z_{pyr}, $g_{B\to O}$; thermodynamic properties permitting Fig. 19 to be drawn; kinetic information enabling the $F(\ldots)$ functions of equations (39) and (40) to be plotted out; and information about the aerodynamics permitting the $F(\ldots)$ function of equation (41) to be computed. Sketches will be used to illustrate the steps.

The first point to note is that specification of the quantities η and $m_{ox,\,3,\,S}/m_{ox,\,S}$ in this situation will specify t_S and f_S; this follows from the geometry of Fig. 19. It follows that, just as equation (39) determines a family of curves on Fig. 20, so do equations (40) and (41); in the latter cases, the parameters are $Z_{pyr}/\dot{m}''_{(2)\to(3),\,T,\,ad}$ and $g_{B\to O}/\dot{m}''_{(2)\to(3),\,T,\,ad}$. The latter families are sketched in Fig. 21.

Now the values of the last two parameters can be deduced from the data of our problem. It follows that, as soon as Fig. 21 has been constructed, the quantity $\dot{m}''$ can be deduced from the ordinate value appropriate to the network point corresponding to the data. The problem is thus solved.

Discussion. Inspection of Fig. 21 shows that, at small values of $g_{B\to O}$, the solution point is near the left hand border: we then have a process which is not controlled by mass transfer at all, but by those discussed in conventional works on solid-propellant combustion [19]. When the mass-transfer conductance is large however,

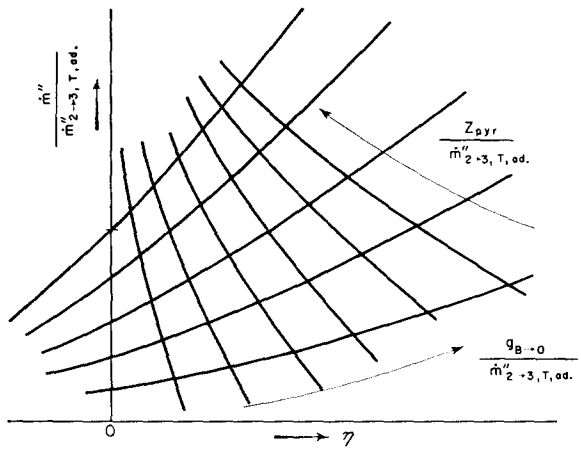

FIG. 21. Graph for determining actual burning rate, given values of the parameters governing surface pyrolysis, mass-transfer conductance and (2) → (3) deflagration.

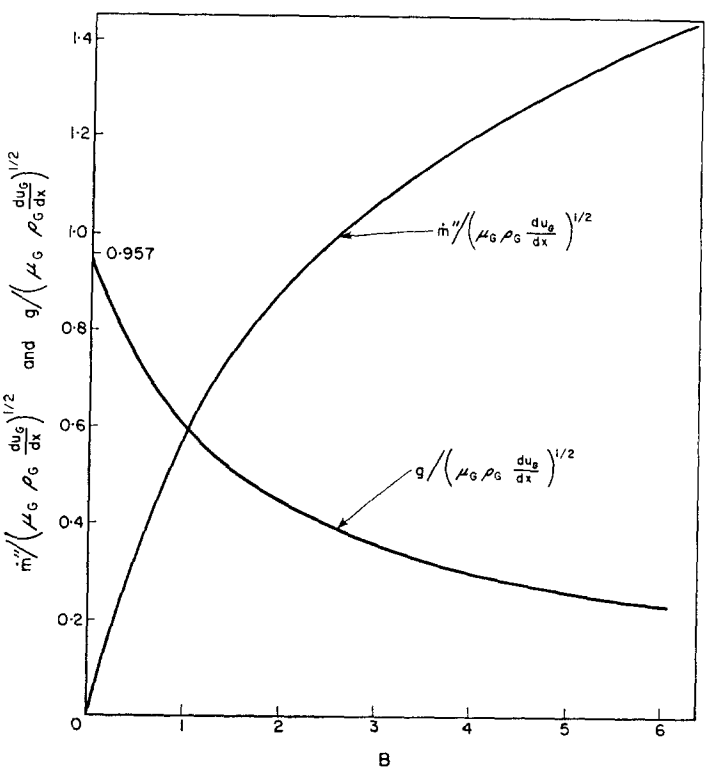

FIG. 22. Curves permitting the calculation of conductance and mass transfer rate at an axi-symmetrical laminar stagnation point, for $\mu/\Gamma = 0{\cdot}7$.

relative to the adiabatic propellant deflagration rate for the pressure and T-state in question, the burning rate increases. At very high values of this dimensionless quantity, the deflagration flame will coalesce with the diffusion flame; in this case the suppositions underlying the above theory, for example Fig. 20, cease to hold, and the situation becomes too complex to be dealt with by the methods of the present paper.

It should be clear that a very similar procedure can be used if it is supposed that the diffusion flame is absent. The procedure is valid also when the gas stream is at such a low temperature as to diminish rather than increase the deflagration velocity (η negative).

4. BOUNDARY-LAYER THEORY FOR LAMINAR AXI-SYMMETRICAL STAGNATION-POINT FLOW

In this section we shall merely present sufficient information about the laminar boundary-layer at an axi-symmetrical stagnation point to permit exemplary mass transfer calculations to be carried out. It suffices therefore to present Fig. 22 which is valid when the Prandtl or Schmidt number, μ/Γ is equal to 0·7.

In Fig. 22, the curve for $\dot{m}''/[\mu_G\ \rho_G\ du_G/dx]^{1/2}$, is taken from Spalding [14] and is based on exact solutions of Howe and Mersman [30] and other authors. It relates the mass transfer rate $\dot{m}''$ to the stream-wise velocity gradient du_G/dx, the driving force B and other quantities. As far as is known, variations in the properties μ, ρ and Γ through the boundary layer do not greatly affect the position of the curve.

The curve for $g/[\mu_G\ \rho_G\ du_G/dx]^{1/2}$ is obtained by dividing the ordinate of Fig. 22 by B; its ordinate is thus a dimensionless form of the conductance g. It will be noted that, as B tends to zero, g tends to the value $0{\cdot}957\sqrt{(\mu_G\ \rho_G\ du_G/dx)}$, but falls below this value as B increases.

It should be clearly understood that, apart from secondary influences brought about by the variations of μ, ρ and Γ with temperature and composition, about which usually only inadequate information is available, the curves of Fig. 22 can be used regardless of whether the process in question is water-vaporization, carbon-combustion, hydrogen-transpiration, silica-pyrolysis, ammonium perchlorate-combustion, or any other mass transfer process.

5. SOME APPLICATIONS OF THE METHOD

In the present section some specific numerical problems will be considered, primarily to remove any doubt about the applicability and usefulness of the methods presented. Of course, absence of kinetic data, and to a lesser extent thermodynamic data, prevent immediate solution of every problem which comes to mind. A subsidiary purpose of the present paper has been to stimulate the search for the missing data, by showing how useful they can be. Incidentally one of the following problems (Section 5.2) concerns the experimental determination of such data.

5.1. *Comparison of water and carbon as nose-cone protectors*

The problem. A nose-cone re-enters the earth's atmosphere. The air between the shock wave and the surface has an enthalpy of 8000 Btu/lb_m (corresponding to a flight speed of 20,000 ft/s) and a pressure of 1 atm. In one possible design, water is supplied, from a reservoir at 60°F, continuously to the surface where it vaporizes. In another possible design, the nose-cone is made of graphite the bulk of which is at 60°F; the graphite burns away steadily.

In which design is the greater weight of protective material consumed?

Solution (a). When radiation is neglected. If radiation is negligible, the O- and T-states are identical (Section 2.2). The problem can then be solved without information concerning the conductance. Referring to the *h-f* chart for H_2O–air at 1 atm pressure (Fig. 4), we see that, with G at: $f = 0$, $h = 8000$ Btu/lb_m, and T at: $f = 1$, $t = 60°F$, and with the assumption that S lies on the equilibrium line, we have:

S lies at: $f = 0{\cdot}876$, $h = 1018$ Btu/lb_m and the driving force, $B = 7{\cdot}05$.

Referring in the same way to the *h-f* chart for carbon–air at 1 atm pressure (Fig. 9), and assuming that the S-state is an equilibrium one, we find:

S lies at $f = 0{\cdot}28$, $h = 7000$ Btu/lb_m and the driving force, $B = 0{\cdot}39$.

Clearly the rate of water consumption will be greater than the rate of carbon consumption, because its driving force is so much greater. To determine the ratio of the rates we turn to Fig. 22,

which shows that this is approximately equal to 1·5/0·29, i.e. to 5·18. We conclude that more than five times as much water is required as carbon.

Comments. Of course it must be recognized that the water keeps the surface temperature down to about 212°F whereas the carbon surface temperature exceeds 7500°F; the high internal energy of the heated layer of carbon may lead to difficulties due to "heat soakage" at the termination of flight.

Alternatively one might envisage allowing the surface temperature to rise above the boiling point of water by reducing the water supply rate so that vaporization occurs within the porous material below the surface. In this way it might be permissible to allow t_S to rise to 2000°F. Inspection of the *h-f* chart of Fig. 4 shows that the driving force B would fall to 3·62. However this would still not enable the water system to compete with carbon; moreover the system envisaged would be almost impossible to control.

Solution (b). When radiation is accounted for. Radiation from a water surface at 212°F is probably negligible; not however that from carbon at more than 7500°F abs. We shall now consider the effect of radiation from the carbon, supposing it to be at the black-body rate given by:

$$\dot{q}''_{\text{rad}} = \sigma T_S^4 \qquad (42)$$

where σ = Stefan's Constant = $0{\cdot}1713 \times 10^{-8}$ (Btu/ft²h (°F abs.)⁴);

T_S = absolute temperature of surface (°F abs.).

To proceed further, we have to be able to calculate absolute values of the mass transfer rate. Let us suppose that du_G/dx in the vicinity of the stagnation point has the reasonable value of $1{\cdot}8 \times 10^7$ h^{-1} and that the product $\mu_G \rho_G$ has the value $1{\cdot}5 \times 10^{-3}$ lb$_m^2$/ft⁴h. Then $\sqrt{(\mu_G \rho_G \, du_G/dx)}$ is equal to: 164 lb$_m$/ft²h. Thus if the driving force B were 0·39, the mass transfer rate would, according to Fig. 22, be $0{\cdot}29 \times 164 = 47{\cdot}6$ lb$_m$/ft²h.

Now at a temperature of 7500°F abs., evaluation of equation (42) shows that the radiative heat flux is $5{\cdot}28 \times 10^6$ Btu/ft²h. Therefore the reduction in the enthalpy of the transferred substance due to radiation is $5{\cdot}28 \times 10^6 \div 47{\cdot}6 = 1{\cdot}11 \times 10^5$ Btu/lb$_m$. Evidently our assumption that states O and T are identical was unjustified. The surface temperature now has to be found by the trial and error procedure outlined in Section 2.2. A quick calculation of this character shows that it must be about 5500°F abs., and that the corresponding driving force, B, is 0·174.

We conclude that in this case the radiation from the carbon surface results in a lowering of the surface temperature of more than 2000°F, and a reduction of B from 0·39 to 0·174. The latter effect is the more important, for it means that the weight of the heat-shield material is approximately halved; carbon is now about *ten* times as good as water in protecting the missile. Incidentally, it should be noted that $B = 0{\cdot}174$ corresponds to a location of S on the upper vertical portion of the S-line of Fig. 9; carbon vapour is absent from the S-state, and carbon monoxide is the only oxide.

Reaction-kinetic effects. The calculations just made have assumed equilibrium to prevail at the surface, in concluding the discussion of this problem, let us examine whether the assumption is reasonable.

Reference to the conclusions of Section 3.1 above confirms that the assumption is reasonable in the case of water vaporization. Reference to Section 3.2 shows that the assumption is also reasonable for carbon combustion if the following quantity is considerably less than unity:

$$\frac{g\sqrt{(2\pi k_{\text{ox, s}})}}{\rho_S a_{\text{ox, s}}} \exp(E/\mathscr{R} T_S).$$

Now in our problem we have:

$g \approx 160$ lb$_m$/ft²h;

$k_{\text{ox, s}} \approx 1{\cdot}25$;

$\rho_S \approx 0{\cdot}008$ lb$_m$/ft³;

$a_S \approx 9 \times 10^6$ ft/h;

$T_S \approx 5500$°F abs.

Taking also $E = 45{,}000$ Btu/lb mole, we thus determine that the above expression has the value 0·056.

We conclude that the rough kinetic data

currently available indicate that the rate of chemical reaction at the surface will indeed be fast enough for the S-state to be substantially in equilibrium in our example. It should be noted that, if more precise knowledge of the kinetic constants should indicate that this is not the case, the effect will be to reduce the driving force, and so the burning rate, still farther below the values calculated above. Anything that can be done to render the carbon unreactive is advantageous as far as reducing the heat-shield weight is concerned.

5.2. *Determination of the reaction-rate constants for carbon in air*

Problem. It is desired to establish whether the reaction-rate constants of a given sample of graphite are such as to reduce the burning rate below that calculated in the last example. How can a simple experiment be devised to determine this?

This problem may be re-phrased as follows:

Determine experimentally the value of $\{\rho_S a_{ox,\,s}/\sqrt{(2\,\pi\,k_{ox,\,s})}\}.\ \exp\,(-\,E/\mathscr{R}\,T_S)$ for the graphite in question where T_S is around 5500°F abs. and the pressure is atmospheric. Then compare the value of this quantity with the expected value of the mass-transfer conductance g, namely 160 lb_m/ft^2h.

Solution. The following experiment would suffice:

(i) Set up an apparatus such as is shown in Fig. 2, with the graphite in question as the specimen of reactive material. The gas emerging from the nozzle should contain oxygen.

(ii) Adjust the temperature and oxygen content of the gas stream, the temperature of the surroundings with which the reactive surface is in radiative communication, and the supply temperature of the graphite, so that the surface temperature is in the neighbourhood of 5500°F abs. (measured optically, or calculated using the techniques of the present paper).

(iii) Vary the conductance g by changes to the flow velocity of the gas and the diameter of the nozzle, and measure the corresponding variations of burning rate. g should be increased to well above the value to be encountered in the full-scale operation, viz. about 160 lb_m/ft^2h.

(iv) *Qualitative interpretation.* If the burning rate $\dot{m}''$ remains proportional to g within the whole range of measurement, the chemical reaction rate can be regarded as sufficiently fast to impose no limitation on the burning rate, the S-state is in equilibrium as postulated in Section 5.1. If $\dot{m}''$ increases less rapidly than g, on the other hand, reaction–kinetic limitations are present.

(v) *Quantitative interpretation.* Knowledge of $\dot{m}''/g$, i.e. of the driving force B signifies knowledge of the point at which the S-line crosses the isotherm in question on the h-f diagram, and hence, $m_{ox,\,s}$. Insertion of this quantity in equation (33), or a modification thereof, leads to a solution of the problem.

Discussion. The ways in which the suggested procedure can be modified and extended are too numerous and obvious to be worth enumerating in detail. However the following remarks might be noted:

(i) If it is not possible to detect reaction–kinetic effects at the temperature specified, it may be desirable to lower the surface temperature until such effects are measurable. Indeed it will normally be advantageous to pursue the investigation to the point at which it is possible to specify the activation energy and the dependence of the burning rate on $m_{ox,\,s}$. The relation between $\dot{m}''$, $m_{ox,\,s}$, and T_S may fit the framework of equation (31) or it may not; only experiment can decide.

(ii) However, provided that a satisfactory theoretical framework exists, it is *not* necessary to duplicate full-scale (i.e. heat-shield) conditions in order to obtain the desired information. This is perhaps the most useful lesson which can be learned from consideration of the present example.

(iii) It is important to ensure that, if the diffusion flame burning carbon monoxide

and oxygen exists in the full-scale, it should also exist in the laboratory test. This can be ensured by having a sufficiently hot gas supply. The presence of a small amount of water vapour in the supply stream will probably also be helpful.

5.3. *Analysis of an experiment with ammonium perchlorate and methane*

Problem. In an apparatus such as that shown in Fig. 2, the reactive solid material is ammonium perchlorate and the gas stream consists of methane at atmospheric pressure and temperature. In a particular experiment,* the following measurements are made:

$u_\infty = 1093$ cm/s;

$D = 0{\cdot}95$ cm;

$\dot{m}'' = 0{\cdot}1$ g/cm² s.

Determine the mass transfer driving force B, and comment on whether the burning rate is primarily controlled by the deflagration characteristics of the solid propellant or by the properties of the methane stream.

Solution. Tables of gas properties show:

$$\mu\rho \approx 2{\cdot}1 \times 10^{-7}\ \text{g}^2/\text{cm}^4\ \text{s}.$$

Hence, and from equation (2) and the data:

$$\sqrt{(\mu\rho\, du_G/dx)} = 1{\cdot}55 \times 10^{-2}\ g/\text{cm}^2\ \text{s}.$$

and

$$\dot{m}''/\sqrt{(\mu\rho\, du_G/dx)} = 6{\cdot}45.$$

Inspection of Fig. 22 shows that this ordinate occurs at a value of the abscissa lying right off the scale. We can merely conclude that the driving force B is greater than, say, 30.

As to whether the deflagration or the boundary-layer processes are dominant in this situation, we can make the following deductions:

(i) Since B is large, f_S is close to unity.

(ii) Therefore, since t_S must be considerably in excess of t_{T_2}, for a finite surface pyrolysis rate with an endothermic (1) → (2) reaction, the line marked (iii) in Fig. 19 must be steep.

(iii) Consequently the quantity η, which measures the effect of the boundary-layer-induced enthalpy gradient on the (2) → (3) deflagration, and which is equal to the ratio of the slope of the line marked (ii) in Fig. 19 to that marked (iii), must be very small.

(iv) We conclude that the boundary-layer phenomena are not greatly influencing the burning rate.†

6. CONCLUSIONS

(a) Mass transfer processes in which thermodynamic equilibrium does not prevail adjacent to the phase interface can be analysed by the same methods as those processes for which equilibrium does prevail; any differences in the situations are accounted for by a shift of the location of the line on the enthalpy–composition diagram which represents the mixture states adjacent the interface (S-line).

(b) Whereas a single S-line represents the equilibrium situation (for a given pressure), a family of S-lines has to be considered for the non-equilibrium situation; the parameter is a dimensionless quantity (K_{vap}, K_{ox}, K_{pyr}, etc.) measuring the ratio of the magnitude of the mass-transfer conductance to a molecular flux.

(c) When the phase change is a physical process, without chemical transformations, it appears that departures from equilibrium are only likely to occur under conditions such that the molecular mean free path is of the same order of magnitude as the apparatus dimension.

(d) When the phase change involves a chemical reaction, as in carbon combustion or ammonium chloride pyrolysis, deviations

* Performed by Dr. R. Friedman, Atlantic Research Corporation Alexandria, Va. (Private communication.)

† Friedman's data indeed show that increases of methane blowing rate scarcely affect the burning rate. However *reductions* of methane rate do reduce $\dot{m}''$; indeed the ammonium perchlorate will not burn at all at 1 atm in the absence of methane. The explanation is probably that, at low pressure, radiation loss becomes important; specifically, radiation makes the T-state depend on $\dot{m}''$ and so makes the interactions more complex than would appear from the discussion of Section 3.4.

from equilibrium can be large at low temperatures.

(e) The methods of analysis can be extended to situations such as the burning of ammonium perchlorate in a fuel gas stream, where a gaseous deflagration takes place in addition to the surface pyrolysis and a gaseous diffusion flame, by incorporation of some results of the theory of flame propagation in the presence of an enthalpy gradient.

(f) The prediction of the mass transfer behaviour of materials under conditions of re-entry of the earth's atmosphere can be easily made provided that the appropriate thermodynamic and kinetic data are known. The latter can be determined from measurements made in laboratory-scale apparatus and interpreted through mass transfer theory.

REFERENCES

1. D. B. SPALDING, The combustion of liquid fuels. *Fourth Symposium on Combustion*, p. 847. Williams and Wilkins, Baltimore (1953).
2. F. BOŠNJAKOVIĆ, *Wärmediagramme für Vergasung, Verbrennung und Russbildung*. Springer, Berlin (1956).
3. G. W. SUTTON, Combustion of a gas injected into a hypersonic boundary layer. *Seventh Symposium on Combustion*, p. 539. Butterworths, London (1959).
4. C. M. TU, H. DAVIS and H. C. HOTTEL, Combustion rate of carbon. *Industr. Engng Chem.* **26**, 749 (1934).
5. D. B. SPALDING, *Some fundamentals of combustion*. Butterworths, London (1955).
6. E. WICKE, Contributions to the combustion mechanism of carbon. *Fifth Symposium on Combustion*, p. 245. Reinhold, New York (1955).
7. L. N. KHITRIN, Fundamental principles of carbon combustion and factors intensifying the burning of solid fuels. *Sixth Symposium on Combustion*, p. 565. Reinhold, New York (1957).
8. D. B. SPALDING, A standard formulation for the steady convective mass-transfer problem. *Int. J. Heat Mass Transfer*, **1**, 192 (1960).
9. D. B. SPALDING, Graphical method of calculating heat transfer, condensation and vaporisation rates in processes involving water–steam–air mixtures. *Proc. Inst. Mech. Engng*, **172**, 839 (1958).
10. F. BOŠNJAKOVIĆ, Halbwertgrösse als Bemessungseinheit bei stationärem Austausch. *Chem.-Ing.-Tech.* **29**, 187 (1957).
11. F. BOŠNJAKOVIĆ, Wärme- und Stoffaustausch bei feucheten Gasen. *Kältetech.* **9**, 266; **10**, 309 (1957).
12. F. BOŠNJAKOVIĆ, Austauschvergänge beim lufthaltigen Dampf. *Kyltek. Tidskr.* **3**, 142 (1957).
13. D. B. SPALDING, Adiabatic wall temperature due to mass-transfer cooling with a combustible gas. *J. Amer. Rocket Soc.* **29**, 666 (1959).
14. D. B. SPALDING, Heat and mass transfer in aeronautical engineering. *Aero. Quart.* **11**, 105 (1960).
15. D. B. SPALDING and R. D. TYLER, *Joint Conf. on Thermodynamic and Transport Properties of Fluids, Session* 1, Instn. Mech. Engrs. (1957).
16. T. Y. LI and R. E. GEIGER, Stagnation point of a blunt body in hypersonic flow. *J. Aero. Sci.* **24**, 25 (1957).
17. A. LECLERC, Déviation d'un jet liquide par une plaque normale à son axe. *Houille Blanche*, 5th year, nr. 6, 3 (1950).
18. D. B. SPALDING, Conserved-property diagrams for rate-process calculations. Parts I and II. *Chem. Engng Sci.* **11**, 183 and 225 (1960).
19. D. B. SPALDING, The theory of burning of solid and liquid propellants. *Combustion and Flame*, **4**, 59 (1960).
20. A. BUSEMANN, *Der Wärme- und Stoffaustausch*. Springer, Berlin (1933).
21. H. A. BETHE and M. C. ADAMS, A theory for the ablation of glassy materials. *J. Aero. Space Sci.* **26**, 321 (1959).
22. J. ADLER and D. B. SPALDING, One-dimensional laminar flame propagation with an enthalpy gradient. *Proc. Roy. Soc.* A. (1961). To be published.
23. S. M. SCALA and G. L. VIDALE, Vaporization processes in the hypersonic laminar boundary layer. *Int. J. Heat Mass Transfer*, **1**, 4 (1960).
24. D. B. SPALDING, The stability of exothermic chemical reactions in simple non-adiabatic systems. *Chem. Engng Sci.* **11**, 53 (1959).
25. J. S. BINFORD, Kinetics of oxidation of graphite. *Literature of the combustion of petroleum*, p. 39. Amer. Chem. Soc. Washington (1958).
26. Y. B. ZELDOVICH, The theory of combustion of initially unmixed systems. *J. Tech. Phys.* **19**, (1949), transl. as NACA TM 1296 (1951).
27. D. B. SPALDING, A theory for the extinction of diffusion flames. *Fuel*, **33**, 253 (1954).
28. R. D. SCHULTZ and A. O. DEKKER, The absolute thermal decomposition rates of solids. *Fifth Symposium on Combustion*, p. 260. Reinhold, New York (1955).
29. G. ROSEN, Burning ratio of solid propellants. *J. Chem. Phys.* **32**, 89 (1960).
30. J. T. HOWE and W. A. MERSMAN. *Solutions of the laminar compressible boundary-layer equations with transpiration which are applicable to the stagnation regions of axi-symmetric blunt bodies*. NASA TN D-12 (1959).